International Applied Mechanics, Vol. 45, No. 1, 2009

USING MESH-BASED METHODS TO SOLVE NONLINEAR PROBLEMS OF STATICS FOR THIN SHELLS

V. A. Maksimyuk[*], E. A. Storozhuk[*], and I. S. Chernyshenko[**]

The paper outlines a numerical procedure for solving physically and geometrically nonlinear problems of statics for thin shells based on three mesh-based methods: finite-difference, variational difference, and finite-element methods. The methodological, algorithmic, and analytical aspects of implementing the Kirchhoff–Love hypotheses are analyzed. The algorithmic approach employs Lagrangian multipliers. The advantages and disadvantages of these methods are evaluated

Keywords: finite-difference method, variational difference method, finite-element method, Kirchhoff–Love hypotheses, Lagrangian multipliers, nonlinear elastic composite, elastoplastic state

Introduction. Strength analysis of structural members such as shells of complex geometry is mainly conducted on a computer using numerical mesh-based methods, including the finite-difference method (FDM), the variational difference method (VDM), and the finite-element method (FEM). To derive the basic equations of the theory of thin shells, it is sufficient to use the classical model based on the Kirchhoff–Love hypotheses. The Kirchhoff–Love kinematics is implemented differently in these three methods.

The system of governing equations in the FDM is known to be derived from the equilibrium equations for an element of the shell, while the Kirchhoff–Love constraints are incorporated analytically, by substituting the corresponding relations into the formulas describing the distribution of displacements throughout the thickness of the shell. This way causes no complications.

Contrastingly, the system of governing equations in the VDM and FEM is derived from the extremum condition for some functional. An attempt to implement Kirchhoff–Love constraints analytically gives rise to higher-than-first-order derivatives of displacements in the functionals. Note that the complications in the VDM are only restricted to more awkward equations and the necessity of deriving them because the VDM imposes no special requirements upon the smoothness of the integrands and functions. In the FEM, however, certain requirements are placed upon the smoothness of the coordinate functions, and the construction of an element is complicated if the integrands include higher-order derivatives.

These circumstances led to a search for alternative ways of incorporating the Kirchhoff–Love constraints such as those that would not produce derivatives of higher than the first order in the integrands. Noteworthy are two groups of approaches that employ Lagrangian multipliers and penal functions. Applying them requires certain correctness [17, 52] associated with the variation order and additional conditions.

However, the use of Lagrangian multipliers to implement the Kirchhoff–Love hypotheses increases the number of varied functions and requires much computing. This is obviously why the Kirchhoff–Love constraints were first (1967) used [46] in the FEM for a plate by specifying them at discrete points of an element (discrete Kirchhoff element). Later, this method was extended to thin shells [45, 70] and is widely used now [26, 71] within the framework of the so-called discrete Kirchhoff theory (DKT). A somewhat different approach was employed in [37], where the Dirac delta function was used to interpolate Lagrangian multipliers. Similar results were obtained in [30–33, 43, 64] without delta function. In the VDM, Lagrangian

S. P. Timoshenko Institute of Mechanics, National Academy of Sciences of Ukraine, 3 Nesterov St., Kyiv, Ukraine 03057, e-mail: [*]desc@inmech.kiev.ua, [**]prikl@inmech.kiev.ua. Translated from Prikladnaya Mekhanika, Vol. 45, No. 1, pp. 41–70, January 2009. Original article submitted January 11, 2008.

 1063-7095/09/4501-0032

multipliers were first used to implement the Kirchhoff–Love hypotheses in [8] and then successfully used in [17, 18, 52] to solve linear and nonlinear problems.

There is an alternative approach that uses shear models to design thin shells and abandons [7, 28, 59] or partially adopts the Kirchhoff–Love hypotheses. However, an attempt to directly apply shear FE models to thin-walled structures encounters so-called shear locking [26, 52, 69], which slows down the convergence of numerical methods, and the partial implementation of the hypotheses should be justified appropriately. The approaches to solving this and related problems are classified in [69].

Note that the VDM and FEM and associated software are developed based on variational principles traditionally in two stages: analytic and algorithmic. The analytic stage involves the selection of a variational principle; the selection of varied functions; the consideration of the dimension of the problem, hypothetical simplifications, and a priori information on expected solutions; the establishment of the relationships between the functions chosen; incorporation of these relationships analytically or using Lagrangian multipliers; possible elimination of some Lagrangian multipliers; discretization of the problem; and variation of the functional. The algorithmic stage involves the derivation and numerical solution of the system of governing algebraic equations. Note that in the calculus of variations, it is generally incorrect to introduce any relationships among the varied functions after the variation of the functional. It is for this reason that the two stages are separated after the variation.

In this context, some methods for the overcoming of locking (reduced integration and the like) and the partial incorporation of the Kirchhoff–Love hypotheses may be considered heuristic. Such methods were not universal and sometimes produced erroneous solutions. Some of such shortcomings were indicated in [26, 135] and in the literature referenced therein. The reason is apparently that the stages overlap and, thus, the requirement of the calculus of variations that no relationships should be introduced after variation is not met. The correct [17–19, 52] use of the Lagrangian multiplier method for the implementation of the Kirchhoff–Love hypotheses based on mixed functionals is universal and produces correct solutions.

There are numerical analytical [60], meshfree [36, 47], and other [27, 58] methods free from these shortcomings.

Here we generalize the results of the studies that have been performed under the leadership of Academician A. N. Guz at the Department of Dynamics and Stability of Continua of the S. P. Timoshenko Institute of Mechanics for four decades. These studies involved the development of mesh-based methods for stress–strain analysis of thin nonlinear elastic composite and elastoplastic isotropic shells. Emphasis was on stress concentration in complex shells weakened by curvilinear holes.

Note that the paper [42] was the first to point to the necessity of allowing for physical and geometrical nonlinearities in the stress–strain analysis of shells with holes.

Pioneering theoretical studies into the SSS of elastoplastic shells of revolution with finite deflections based on the FDM date back to 1966 [29]. The further development of this method is reflected in [13, 24, 41, 52]. Shells of revolution made of nonlinear elastic orthotropic materials were considered in 1986 [35], and allowance for physical and geometrical nonlinearities was made in 1988 [55]. The basic results obtained with the FDM in the axisymmetric case are presented in Sec. 1. Two-dimensional problems are addressed in Secs. 2–4. The methods outlined in Secs. 2 and 3 are applicable to domains with four corner points, while the modified FEM described in Sec. 4 is free from such a restriction.

1. Finite-Difference Method. The method of deriving and solving nonlinear governing equations for thin shells made of isotropic materials is well developed [41, 68]. As far as physically nonlinear anisotropic composites are concerned, there are difficulties associated with the theoretical description of the nonlinear deformation of composites, the experimental determination of the quantities and functions used by the theory, and the establishment of the explicit stress–strain relationship. The basic results on nonlinear elastic orthotropic shells of revolution are outlined below with emphasis on the methodical aspects [13, 20, 35, 40, 41, 54, 55].

1.1. Problem Formulation and Basic Equations. Consider a thin deep shell of varying thickness made of a nonlinear elastic orthotropic composite. The loading process occurs under surface and boundary forces and at constant temperature and is active and simple [16]. The axes of orthotropy of the composite are aligned with the lines of principal curvature of the shell and the axes of the orthogonal curvilinear coordinate system (s, θ, γ) used to describe the shell (Fig. 1). At certain levels of the load, the shell exhibits the nonlinear properties of an anisotropic material at which displacements along the normal to the shell surface are comparable with or much greater than its thickness, though strains are small. These facts allow us to use the geometrically nonlinear second-order theory of shells [21, 24] and the theory of anisotropic plasticity [15, 16, 40] to derive the governing equations.

Then the strains at an arbitrary point of the shell ($\gamma = \text{const}$) are expressed by the formulas

$$e_s = \varepsilon_s + \gamma\kappa_s, \qquad e_\theta = \varepsilon_\theta + \gamma\kappa_\theta \tag{1.1}$$

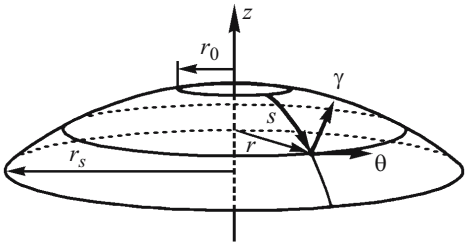

Fig. 1

in terms of the strains of its midsurface:

$$\varepsilon_s = u' + \kappa_s w + \frac{1}{2}\theta^2, \qquad \varepsilon_\theta = B^* u + \kappa_\theta w,$$

$$\kappa_s = k_s' u - k_s^2 w - w'', \qquad \kappa_\theta = k_\theta' u - k_\theta^2 w - B^* w', \tag{1.2}$$

where u and w are the displacements along the coordinate axes (s, γ); $\theta = k_s u - w'$ is the angle of rotation of the normal around the axis (coincides with the angle of rotation of the tangent to the s-axis in the case of the Kirchhoff–Love hypotheses); k_ρ $(\rho = s, \theta)$ are the principal curvatures; $B^* = B'/B$, $B^{**} = B''/B$, $B = r$ is the parallel circle radius; and $(')$ denotes differentiation with respect to s. Note that formulas (1.1) and (1.2) partially incorporate the change of the metrics throughout the thickness of the shell.

If the stress state is plane and loading is simple, the strain components are nonlinearly expressed in terms of the stress components as

$$e_s = \frac{1}{E_s}(\sigma_s - \nu_s \sigma_\theta) + \Psi(q_{ss}\sigma_s + q_{s\theta}\sigma_\theta) \quad (s \leftrightarrow \theta), \tag{1.3}$$

where E_s, E_θ, ν_s, and ν_θ are the elastic constants of an orthotropic composite; $\Psi(f)$ is a function describing the nonlinear deformation of the composite; q_{ss}, $q_{\theta\theta}$, and $q_{s\theta}$ are the components of the tensor responsible for the anisotropy of the composite; and $f = (q_{ss}\sigma_s^2 + q_{\theta\theta}\sigma_\theta^2 + 2q_{s\theta}\sigma_s\sigma_\theta)/2$ is a quadratic stress function.

The constants and function in (1.3) are determined in tests on composite samples subject to tension along the axes of orthotropy and at an angle of 45° to them. An experimental procedure and a data processing technique were proposed in [16] and improved in [13, 40].

Equations (1.3) are essentially nonlinear. Unlike the equations of the deformation theory of isotropic plasticity, they are analytically unresolvable for the stresses. They can be resolved numerically, using, for example, Newton's method [53], which will be detailed in Sec. 3 for the more general case of two-dimensional problems. After numerical inversion of (1.3), we have

$$\sigma_s = \sigma_s(e_s, e_\theta) \quad (s \leftrightarrow \theta), \tag{1.4}$$

where we can separate out nonlinear (σ_s^*) and linear (σ_s^0) terms:

$$\sigma_s^* = \sigma_s - \sigma_s^0 \quad (s \to \theta). \tag{1.5}$$

Equations (1.4) and (1.5) and all the subsequent ones that include the total stresses σ_s and σ_θ or their nonlinear components σ_s^* and σ_θ^* should be considered as approximate formulas rather than analytic expressions. Contrastingly, the formulas for the linear stress components are analytic:

$$\sigma_s^0 = \frac{E_s}{1 - \nu_s \nu_\theta}(e_s^0 + \nu_\theta e_\theta^0) \quad (s \leftrightarrow \theta),$$

which include the strain components and where $e_s^0 = e_s - \theta^2/2$, $e_\theta^0 = e_\theta$.

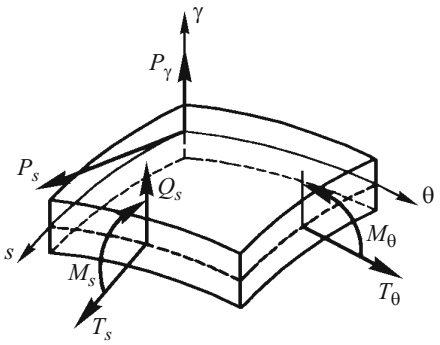

Fig. 2

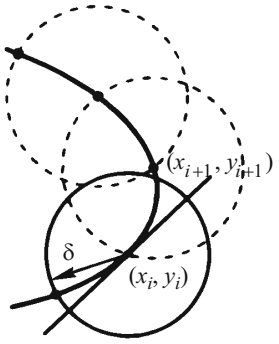

Fig. 3

Note that Eqs. (1.3) yield, as a special case, the constitutive equations for a linear elastic orthotropic material [14] if $\Psi = 0$ and the constitutive equations for an isotropic incompressible elastoplastic ($E_s = E_\theta = E$) material Q_s if $\nu_s = \nu_\theta = \nu = 0.5$, $q_s = q_\theta = 2$, $q_{s\theta} = -1$, $f = \sigma_i^2$, $\Psi = \omega_i / 2E(1-\omega_i)$, where ω_i is the plasticity function and σ_i is stress intensity.

We now introduce thickness-average internal (Fig. 2) forces T_s, T_θ and moments M_s, M_θ, which have, according to (1.5), linear and nonlinear components. Applying the displacement method [24], we obtain a system of nonlinear differential equations of the sixth order with variable coefficients:

$$\sum_{j=0}^{2} a_{ij} u^{(j)} + \sum_{j=0}^{4} b_{ij} w^{(j)} + (\Omega_i + P) D_s^{-1} = 0 \quad (i = 1, 2), \tag{1.6}$$

where a_{ij} and b_{ij} are variable coefficients obtained [54] using the linear theory of thin orthotropic shells of revolution of varying thickness $h = h(s)$; $P_i(s) = P_\rho(s)$ are the components of the surface load vector; $D_s = E_s h^3 / 12(1-\nu_s\nu_\theta)$, Ω_i are nonlinear terms,

$$\Omega_1 = (T_s^*)' + B^*(T_s^* - T_\theta^*) + k_s Q_s^*, \quad \Omega_2 = B^* Q_s^* + (Q_s^*)' - k_s T_s^* - k_\theta T_\theta^*. \tag{1.7}$$

The variables appearing in (1.7) are defined by the formulas

$$Q_s^* = B^*(M_\theta^* - M_s^*) + (M_s^*)' - T_s\theta, \quad T_s^* = \int_{-h/2}^{h/2} \sigma_s^* d\gamma, \quad M_s^* = -\int_{-h/2}^{h/2} \sigma_s^* \gamma d\gamma \quad (s \to \theta).$$

To solve applied problems for open shells of revolution, the equilibrium equations (1.6) should be supplemented with boundary conditions [24].

1.2. Solution Technique. The technique of solving nonlinear problems is based on the method of successive approximations and FDM [13, 24]. It appears that the simple iteration method is quite acceptable for not very flexible shells [54, 55].

The algorithm of solving such (non)linear problems is based on the numerical discretization of a plane curve $F(x, y) = 0$. The reason is that the coordinate (s) that measures the arc length of the meridian is reckoned in the midsurface of the shell. For some noncanonical domains (say, an ellipsoid [39]), the coefficients of the quadratic forms of the surface are not expressed explicitly in terms of this coordinate. The numerical discretization algorithm [34] for a curve in a Cartesian coordinate system (x, y) is as follows.

Consider a point $M_1(x_1, y_1)$ on the curve. It is necessary to find a point $M_n(x_n, y_n)$ on this curve such that the arc length M_1M_n is equal to a preset value. To this end, we use the tangent method to divide the arc M_1M_n by n points spaced by a small interval δ. After that, the arc is replaced by a tangent segment near the nodal points. The numerical discretization of a plane curve is schematized in Fig. 3.

TABLE 1

Problem	p_0	$\widetilde{w}$	σ_θ^+	σ_θ^0	σ_θ^-
LP	15	0.392	1668	1359	1050
PNP	15	0.467	1430	1236	1008
GNP	15	0.362	1557	1299	1041
GNP	–15	–0.439	–1848	–1433	–1017
PGNP	15	0.411	1333	1172	988
PGNP	–15	–0.688	–1721	–1397	–965

If some point (x_i, y_i) belongs to a curve, i.e., $F(x_i, y_i) = 0$, then the next point $(x_i + \Delta x_i, y_i + \Delta y_i)$ should satisfy the system of equations

$$\begin{cases} F(x_i + \Delta x_i, y_i + \Delta y_i) = 0, \\ \Delta x_i^2 + \Delta y_i^2 = \delta^2. \end{cases}$$

After expansion of the function F about the point (x_i, y_i), the system becomes

$$\begin{cases} F(x_i, y_i) + \dfrac{\partial F(x_i, y_i)}{\partial x}\Delta x_i + \dfrac{\partial F(x_i, y_i)}{\partial y}\Delta y_i = 0, \\ \Delta x_i^2 + \Delta y_i^2 = \delta^2, \end{cases}$$

whence

$$\Delta x_i = \frac{-FF_x \pm F_y\sqrt{\delta^2(F_x^2 + F_y^2) - F^2}}{F_x^2 + F_y^2}, \quad \Delta y_i = \frac{-FF_y \pm F_x\sqrt{\delta^2(F_x^2 + F_y^2) - F^2}}{F_x^2 + F_y^2}. \tag{1.8}$$

Next, the coordinates of the point $M_n(x_n, y_n)$ are determined by the algorithm

$$x_{i+1} = x_i + \Delta x_i, \qquad (i = \overline{1, n-1}) \qquad (x \to y).$$

Note that the sign in formulas (1.8) represents the direction of tracing a plane curve.

1.3. Stress–Strain Analysis of a Nonlinear Elastic Orthotropic Flexible Spherical Shell. Let us analyze the nonlinear elastic SSS of a flexible spherical shell around a circular hole. The geometrical parameters and mechanical characteristics are the following [24, 55]: $R / h = 62.5$, $r_0 / h = 5$, $E_s = 15$ GPa, $E_\theta = 12$ GPa, $\nu_\theta = 0.12$, $q_{ss} = 2$, $q_{\theta\theta} = 3.14$, $q_{s\theta} = 0.24$. The material of the shell is orthotropic glass-reinforced plastic PN-1, T-1 (see [16] for its nonlinear properties). The shell is subject to a uniformly distributed load $p_\gamma = p_0 \cdot 9.81 \cdot 10^4$ Pa.

We will discuss specific results for thin-walled shells (h = const) subject to internal ($p_0 = 15$) and external ($p_0 = -15$) pressure.

Table 1 summarizes the maximum deflections $\widetilde{w} = w / h$ and hoop stresses on the outside ($\sigma_\theta^+ = \sigma_\theta \cdot 9.81 \cdot 10^4$ Pa), inside (σ_θ^-), and middle (σ_θ^0) surfaces of the shells on the boundary of the nonreinforced hole. The meridian $s_k / h = 10$ is divided by $k = 160$ nodal points. The relative error achieved in successive approximations of the maximum strains is $\varepsilon = 0.001$. The results

have been obtained by solving linear elastic (LE), physically nonlinear (PNP), geometrically nonlinear (GNP), and physically and geometrically nonlinear (PGNP) problems.

These results allow us to assess the effect, both individual and collective, of nonlinear factors on the stress–strain state of the shells.

1.4. Flow Theory in the Stress–Strain Analysis of Orthotropic Shells of Revolution. The above presentation is based on the assumption of simple loading and the finite stress–strain relation (1.3). It is of interest to solve such problems by using flow theory [15].

The nonlinear incremental constitutive equations of the theory of anisotropic plasticity [15] are algebraically invertible at preset finite stresses, unlike finite relations (1.3). Let us express [56] the stress differentials in terms of the strain differentials, similarly to the linear equations of the theory of anisotropic shells:

$$d\sigma_s = \frac{E_s^+}{1-\nu_s^+\nu_\theta^+}(de_s + \nu_\theta de_\theta) \quad (s \leftrightarrow \theta), \tag{1.9}$$

where

$$E_s^+ = \frac{E_s}{1+\dfrac{E_s W_p'}{2f}(q_s\sigma_s + q_{s\theta}\sigma_\theta)^2},$$

$$\nu_s^+ = \frac{E_s^+}{E_s}\left[\nu_s - \frac{E_s W_p'}{2f}(q_s\sigma_s + q_{s\theta}\sigma_\theta)(q_\theta\sigma_\theta + q_{s\theta}\sigma_s)\right] \quad (s \leftrightarrow \theta). \tag{1.10}$$

The method of incremental loading [2] can be used to reduce the nonlinear problem to a sequence of linear problems with variable elastic parameters E_ρ^+ and ν_ρ^+ $(\rho = s, \theta)$, which depend on the variables s and γ as in an inhomogeneous orthotropic shell of variable stiffness. Here the method of variable elastic parameters is applied during incremental loading.

It is also possible to use the method of elastic solutions during incremental loading. This approach allows us to employ the nonlinear governing equations for a homogeneous orthotropic shell. In this case, the stress increments can be represented as

$$\Delta\sigma_s = \Delta\sigma_s^0 + \Delta\sigma_s^* \quad (s \to \theta), \tag{1.11}$$

where

$$\Delta\sigma_s^0 = \frac{E_s}{1-\nu_s\nu_\theta}(\Delta e_s + \nu_\theta \Delta e_\theta) \quad (s \leftrightarrow \theta), \tag{1.12}$$

while the increments of additional stresses are defined by

$$\Delta\sigma_s^* = \frac{E_s^+}{1-\nu_s^+\nu_s^+}(\Delta e_s + \nu_\theta^+ \Delta e_\theta) - \Delta\sigma_s^0 \quad (s \leftrightarrow \theta). \tag{1.13}$$

Here the nonlinear problem is solved by the method of elastic solutions at each step of loading. Equations (1.9), (1.10) or (1.11)–(1.13) are used to modify the above procedure of solving nonlinear problems for orthotropic shells of revolution.

We will analyze [56] the nonlinear SSS around a hole in thin orthotropic spherical shells (bottoms) subject to internal pressure p [MPa] $(0 < p \le 5)$ and shearing force $Q_0 = pr_0/2$ applied to the boundary of the hole, which is reinforced with a linear elastic ring with the following parameters [24]: $\widetilde{F}_k = E_k F_k / E_s r_k^2$, $\widetilde{J}_k = E_k J_k / E_s r_k^4$.

The outer edge $(s = s_N)$ is hinged. The bottom is made of nonlinear elastic glass-reinforced plastic and has the following parameters: $R = 275h$, $r_0 = 0.156R$, $s_N = 50h$, $E_s = 15$ GPa, $E_\theta = 12$ GPa, $\nu_s = 0.12$. The other parameters and functions in (1.10) responsible for the anisotropy of the material are given in [16]. Two rings of different stiffness have been examined [56]: $\widetilde{F}_k = 0.901\cdot10^{-2}$, $\widetilde{J}_k = 0.101\cdot10^{-4}$ (case 1) and $\widetilde{F}_k = 0.18$, $\widetilde{J}_k = 0.203\cdot10^{-3}$ (case 2). We used the second (1.11)–(1.13), more

TABLE 2

p	γ / h	σ_s	σ_θ	σ_s / σ_θ
1	0.5	–34	13	–2.62
	–0.5	369	54	6.83
2	0.5	–69	26	–2.65
	–0.5	721	103	7.00
3	0.5	–115	38	–3.03
	–0.5	1058	146	7.25
4	0.5	–177	48	–3.69
	–0.5	1385	184	7.53
5	0.5	–254	57	–4.62
	–0.5	1699	217	7.72

efficient version of the method of incremental loading with step $\Delta p = 0.25$. Table 2 (case 2) collects the meridional (σ_s) and hoop (σ_θ) stresses [MPa] on the boundary of the hole and the ratio σ_s / σ_θ for different values of load. They have been obtained by solving nonlinear ($2 \le p \le 5$) and linear ($p = 1$) problems.

Note that reinforcing the hole with a ring of low [56] or high (Table 2) stiffness causes redistribution of stresses on the shell surfaces in both nonlinear and linear problems. An increase in the load changes the ratio σ_s / σ_θ, which depends on the stiffness of the reinforcing ring. For example, as the load increases, the stresses σ_s and σ_θ become closer to each other if the ring has low stiffness and become more different if the ring has high stiffness (Table 2).

Comparing the solutions of nonlinear problems obtained using flow theory and finite constitutive equations [56] (the maximum stresses differ by no greater than 1%) leads us to the conclusion that they can be used to solve problems for shells under active loading.

2. Variational Difference Method. Analytic Implementation of the Kirchhoff–Love Hypotheses. The solution of nonlinear two-dimensional problems for plates and shells with holes involves severe mathematical difficulties. They are often solved with variational methods. The boundary-value problem for the differential equilibrium equations for plates and shells is equivalent to the variational problem of finding a stationary value of a functional for which the original differential equations are the Euler–Lagrange equations [1, 5]. In what follows, we will outline the variational difference method [4, 25] as applied to physically and geometrically nonlinear problems for shells where the geometrical Kirchhoff–Love hypotheses are incorporated in a conventional manner (by expressing the angles of rotation of the normal in the formulas for strains in terms of the displacements of the midsurface of the shell [48, 62]).

2.1. Basic Nonlinear Equations for Elastoplastic Isotropic Shells. Consider an arbitrarily shaped thin shell of thickness h subject to surface ($\{p\} = \{p_1, p_2, p_3\}^{\mathrm{T}}$) and boundary ($\{m_{\mathrm{b}}\} = \{T_{\mathrm{b}}, S_{\mathrm{b}}, Q_{\mathrm{b}}, M_{\mathrm{b}}\}^{\mathrm{T}}$) forces. To describe it, we choose an orthogonal curvilinear coordinate system (α_1, α_2, γ) with the α_1- and α_2-axes being not aligned with the lines of principal curvature. Assuming that the strains of the shell are small and the displacements along the normal to its midsurface are comparable with the thickness, we derive the kinematic equations from the nonlinear second-order theory of shells, which is based on the Kirchhoff–Love hypotheses [6, 24]:

$$\varepsilon_{11} = \varepsilon_{11}^0 + \frac{1}{2}\varphi_1^2, \quad \varepsilon_{12} = \varepsilon_{12}^0 + \varphi_1\varphi_2, \quad \varepsilon_{11}^0 = \frac{1}{A_1}\frac{\partial u}{\partial \alpha_1} + \frac{1}{A_1 A_2}\frac{\partial A_1}{\partial \alpha_2} v + k_{11} w,$$

$$æ_{11} = -\frac{1}{A_1}\frac{\partial \varphi_1}{\partial \alpha_1} - \frac{1}{A_1 A_2}\frac{\partial A_1}{\partial \alpha_2}\varphi_2, \qquad \varphi_1 = \frac{1}{A_1}\frac{\partial w}{\partial \alpha_1} - k_{11}u + k_{12}v \qquad (u, 1 \leftrightarrow v, 2),$$

$$\varepsilon_{12}^0 = \frac{A_1}{A_2}\frac{\partial}{\partial \alpha_2}\left(\frac{u}{A_1}\right) + \frac{A_2}{A_1}\frac{\partial}{\partial \alpha_1}\left(\frac{v}{A_2}\right) - 2k_{12}w, \quad 2æ_{12} = -\frac{A_1}{A_2}\frac{\partial}{\partial \alpha_2}\left(\frac{\varphi_1}{A_1}\right) - \frac{A_2}{A_1}\frac{\partial}{\partial \alpha_1}\left(\frac{\varphi_2}{A_2}\right), \tag{2.1}$$

where u, v, and w are the components of the displacement vector; A_1, A_2, k_{11}, k_{22}, k_{12} are the Lamé parameters, curvatures, and twist of the shell's midsurface; and φ_1 and φ_2 are the angles of rotation of tangents to the coordinate lines.

The nonlinear constitutive equations derived from the deformation theory of plasticity [11, 12] considering compressibility beyond the elastic limit have the form

$$\sigma_{11} = \sigma_{11}^0 + \sigma_{11}^{\mathrm{N}}, \quad \sigma_{12} = \sigma_{12}^0 + \sigma_{12}^{\mathrm{N}}, \tag{2.2}$$

where

$$\sigma_{11}^0 = \frac{2G}{1-\nu}[(\varepsilon_{11}^0 + \gamma æ_{11}) + \nu(\varepsilon_{22}^0 + \gamma æ_{22})],$$

$$\sigma_{11}^{\mathrm{N}} = 2G\left[\left(\frac{1-\omega_i}{1-\nu_i} - \frac{1}{1-\nu}\right)e_{11} + \left(\frac{(1-\omega_i)\nu_i}{1-\nu_i} - \frac{\nu}{1-\nu}\right)e_{22} + \frac{1}{2(1-\nu)}(\varphi_1^2 + \nu\varphi_2^2)\right],$$

$$\sigma_{12}^0 = G(\varepsilon_{12}^0 + 2\gamma æ_{12}), \qquad \sigma_{12}^{\mathrm{N}} = -G(\omega_i e_{12} - \varphi_1\varphi_2),$$

$$e_{11} = \varepsilon_{11} + \gamma æ_{11}, \qquad e_{12} = \varepsilon_{12} + 2\gamma æ_{12} \qquad (1 \leftrightarrow 2), \tag{2.3}$$

G and ν are the shear modulus and Poisson's ratio; ω_i and ν_i are the plasticity function and the variable Poisson's ratio [11]; the superscripts "0" and "N" mark the linear and nonlinear terms, respectively.

Using formulas (2.2), we represent the internal forces and moments in the form

$$T_{11} = T_{11}^0 + T_{11}^{\mathrm{N}}, \quad T_{12} = T_{12}^0 + T_{12}^{\mathrm{N}}, \quad M_{11} = M_{11}^0 + M_{11}^{\mathrm{N}}, \quad M_{12} = M_{12}^0 + M_{12}^{\mathrm{N}}, \tag{2.4}$$

where

$$T_{11}^0 = \frac{2Gh}{1-\nu}(\varepsilon_{11}^0 + \nu\varepsilon_{22}^0), \quad T_{12}^0 = Gh\varepsilon_{12}^0, \quad M_{11}^0 = \frac{Gh^3}{6(1-\nu)}(æ_{11} + \nu æ_{22}), \quad M_{12}^0 = \frac{Gh^3}{6}æ_{12}, \tag{2.5}$$

$$T_{11}^{\mathrm{N}} = \int_{-h/2}^{h/2}\sigma_{11}^{\mathrm{N}}d\gamma, \quad M_{11}^{\mathrm{N}} = \int_{-h/2}^{h/2}\sigma_{11}^{\mathrm{N}}\gamma d\gamma \quad (1 \to 2), \quad T_{12}^{\mathrm{N}} = \int_{-h/2}^{h/2}\sigma_{12}^{\mathrm{N}}d\gamma, \quad M_{12}^{\mathrm{N}} = \int_{-h/2}^{h/2}\sigma_{12}^{\mathrm{N}}\gamma\, d\gamma. \tag{2.6}$$

2.2. Numerical Solution of Nonlinear Two-Dimensional Problems for Flexible Shells Subject to Plastic Deformation. The nonlinear governing equations for displacements follow from the Lagrange equation [1, 5]:

$$\delta\Pi = 0, \tag{2.7}$$

where $\Pi = Э - A_p$ is the total energy of the shell, $Э$ is the strain energy of the shell, and A_p is the work done by the external surface and boundary forces.

The procedure of solving these equations, which describe the stress–strain state of shells taking into account both physical and geometrical nonlinearities, is based on the method of successive approximations (simple iterations) in combination with the variational difference method. The linearized total energy of the shell is represented in the following form using Eqs. (2.1)–(2.6) [48, 62]:

$$\Pi^{\mathrm{LN}} = \frac{1}{2}\iint\limits_{\Sigma} (T_{11}^0\varepsilon_{11}^0 + T_{22}^0\varepsilon_{22}^0 + T_{12}^0\varepsilon_{12}^0 + M_{11}^0\text{æ}_{11} + M_{22}^0\text{æ}_{22} + 2M_{12}^0\text{æ}_{12})A_1A_2\,d\alpha_1 d\alpha_2$$

$$+\iint\limits_{\Sigma}\Big[(T_{11}\varphi_1 + T_{12}\varphi_2)\varphi_1 + \big(T_{22}\varphi_2 + T_{12}\varphi_1\big)\varphi_2$$

$$+ T_{11}^{\mathrm{N}}\varepsilon_{11}^0 + T_{22}^{\mathrm{N}}\varepsilon_{22}^0 + T_{12}^{\mathrm{N}}\varepsilon_{12}^0 + M_{11}^{\mathrm{N}}\text{æ}_{11} + M_{22}^{\mathrm{N}}\text{æ}_{22} + 2M_{12}^{\mathrm{N}}\text{æ}_{12}\Big]A_1A_2\,d\alpha_1 d\alpha_2 - A_p. \qquad (2.8)$$

To derive the difference equations, we cover the domain (Σ) with main (i, j) and auxiliary $(i+1/2,\ j+1/2)$ meshes with spacings l_1 and l_2 along the coordinate lines α_1 and α_2 and change over expression (2.8) from derivatives to finite differences and from integration to summation by the rectangle rule.

We use the stationarity conditions for the total energy to derive the system of governing equations at the node (i, j)

$$\sum_{m=i-2}^{i+2}\sum_{n=j-2}^{j+2}\Big[a_{m,n}^{(k)}u(m,n) + b_{m,n}^{(k)}v(m,n) + c_{m,n}^{(k)}w(m,n)\Big] = -\Omega_k - d_k p_k \qquad (k = 1, 2, 3), \qquad (2.9)$$

where $a_{m,n}^{(k)}$, $b_{m,n}^{(k)}$, $c_{m,n}^{(k)}$, and d_k are variable coefficients; Ω_k are the nonlinear terms representing the plastic strains and large deflections.

In the case of shallow thin shells, simplifying the kinematic equations (2.1), we arrive at the system of governing equations (2.9). The nonzero coefficients of the first equation in this system at internal nodes (i, j) are defined by the formulas

$$a_{i,j}^{(1)} = \frac{\psi}{A_1^2 l_1^2}\bigg|_{i+1/2,\,j} + \frac{\psi}{A_1^2 l_1^2}\bigg|_{i-1/2,\,j} - \nu\frac{\partial A_2}{\partial\alpha_1}\frac{\psi}{l_1A_2A_1^2}\bigg|_{i-1/2,\,j}^{i+1/2,\,j} + \left[\left(\frac{\partial A_2}{\partial\alpha_1}\right)^2 + \frac{1-\nu}{2}\left(\frac{\partial A_1}{\partial\alpha_2}\right)^2\right]\frac{\psi}{A_1^2A_2^2}\bigg|_{i,\,j}$$

$$+\frac{1-\nu}{2}\left(\frac{\psi}{A_2^2l_2^2}\bigg|_{i,\,j+1/2} + \frac{\psi}{A_2^2l_2^2}\bigg|_{i,\,j-1/2} + \frac{\partial A_1}{\partial\alpha_2}\frac{\psi}{l_2A_1A_2^2}\bigg|_{i,\,j-1/2}^{i,\,j+1/2}\right),$$

$$a_{i+1,\,j}^{(1)} = -\frac{\psi}{A_1^2l_1^2}\bigg|_{i+1/2,\,j}, \quad a_{i-1,\,j}^{(1)} = -\frac{\psi}{A_1^2l_1^2}\bigg|_{i-1/2,\,j}, \quad a_{i,\,j+1}^{(1)} = -\frac{1-\nu}{2}\frac{\psi}{A_2^2l_2^2}\bigg|_{i,\,j+1/2},$$

$$a_{i,\,j-1}^{(1)} = -\frac{1-\nu}{2}\frac{\psi}{A_2^2l_2^2}\bigg|_{i,\,j-1/2}, \quad b_{i,\,j}^{(1)} = -\frac{1+\nu}{4}\frac{\partial A_1}{\partial\alpha_2}\frac{\psi}{l_1A_2A_1^2}\bigg|_{i-1/2,\,j}^{i+1/2,\,j}$$

$$+\frac{1+\nu}{8}\frac{\psi}{A_1A_2l_1l_2}\bigg|_{i-1/2}^{i+1/2}\bigg|_{j-1/2}^{j+1/2} - \frac{1+\nu}{4}\frac{\partial A_2}{\partial\alpha_1}\frac{\psi}{l_2A_1A_2^2}\bigg|_{i,\,j-1/2}^{i,\,j+1/2} + \frac{1+\nu}{2}\frac{\partial A_1}{\partial\alpha_2}\frac{\partial A_2}{\partial\alpha_1}\frac{\psi}{A_1^2A_2^2}\bigg|_{i,\,j},$$

$$b_{i+1,\,j}^{(1)} = -\frac{\partial A_1}{\partial\alpha_2}\frac{\psi}{l_1A_2A_1^2}\bigg|_{i+1/2,\,j} - \frac{1-3\nu}{8}\frac{\psi}{A_1A_2l_1l_2}\bigg|_{i+1/2,\,j-1/2}^{i+1/2,\,j+1/2},$$

$$b_{i-1,\,j}^{(1)} = \frac{\partial A_1}{\partial\alpha_2}\frac{\psi}{l_1A_2A_1^2}\bigg|_{i-1/2,\,j} + \frac{1-3\nu}{8}\frac{\psi}{A_1A_2l_1l_2}\bigg|_{i-1/2,\,j-1/2}^{i-1/2,\,j+1/2},$$

$$b^{(1)}_{i,\,j+1}=\frac{1-3\nu}{8}\frac{\psi}{A_1A_2l_1l_2}\bigg|^{i+1/2,\,j+1/2}_{i-1/2,\,j+1/2}+\frac{3-\nu}{4}\frac{\partial A_2}{\partial\alpha_1}\frac{\psi}{l_2A_1A_2^2}\bigg|_{i,\,j+1/2},$$

$$b^{(1)}_{i,\,j-1}=-\frac{1-3\nu}{8}\frac{\psi}{A_1A_2l_1l_2}\bigg|^{i+1/2,\,j-1/2}_{i-1/2,\,j-1/2}-\frac{3-\nu}{4}\frac{\partial A_2}{\partial\alpha_1}\frac{\psi}{l_2A_1A_2^2}\bigg|_{i,\,j-1/2},$$

$$c^{(1)}_{i,\,j}=-\frac{(k_{11}+\nu k_{22})\psi}{2A_1l_1}\bigg|^{i+1/2,\,j}_{i-1/2,\,j}+\left[\left(k_{22}+\nu k_{11}\right)\frac{\partial A_2}{\partial\alpha_1}+(1-\nu)k_{12}\frac{\partial A_1}{\partial\alpha_2}\right]\frac{\psi}{A_1A_2}\bigg|_{i,j}+\frac{1-\nu}{2}\frac{k_{12}\psi}{A_2l_2}\bigg|^{i,j+1/2}_{i,j-1/2},$$

$$c^{(1)}_{i+1,\,j}=-\frac{(k_{11}+\nu k_{22})\psi}{2A_1l_1}\bigg|_{i+1/2,\,j},\qquad c^{(1)}_{i-1,\,j}=\frac{(k_{11}+\nu k_{22})\psi}{2A_1l_1}\bigg|_{i-1/2,\,j},$$

$$c^{(1)}_{i,\,j+1}=\frac{1-\nu}{2}\frac{k_{12}\psi}{A_2l_2}\bigg|_{i,j+1/2},\qquad c^{(1)}_{i,\,j-1}=-\frac{1-\nu}{2}\frac{k_{12}\psi}{A_2l_2}\bigg|_{i,j-1/2},\tag{2.10}$$

where $\psi=2GhA_1A_2l_1l_2/(1-\nu)$.

The nonlinear terms of Eqs. (2.9) are defined by

$$\Omega_1=\left(T^{\mathrm{N}}_{22}\frac{\partial A_2}{\partial\alpha_1}-T^{\mathrm{N}}_{12}\frac{\partial A_1}{\partial\alpha_2}\right)\frac{\omega}{A_1A_2}\bigg|_{i,j}-T^{\mathrm{N}}_{11}\frac{\omega}{A_1l_1}\bigg|^{i+1/2,\,j}_{i-1/2,\,j}-T^{\mathrm{N}}_{12}\frac{\omega}{A_2l_2}\bigg|^{i,\,j+1/2}_{i,\,j-1/2},$$

$$\Omega_2=\left(T^{\mathrm{N}}_{11}\frac{\partial A_1}{\partial\alpha_2}-T^{\mathrm{N}}_{12}\frac{\partial A_2}{\partial\alpha_1}\right)\frac{\omega}{A_1A_2}\bigg|_{i,j}-T^{\mathrm{N}}_{12}\frac{\omega}{A_1l_1}\bigg|^{i+1/2,\,j}_{i-1/2,\,j}-T^{\mathrm{N}}_{22}\frac{\omega}{A_2l_2}\bigg|^{i,\,j+1/2}_{i,\,j-1/2},$$

$$\Omega_3=\left(k_{11}T^{\mathrm{N}}_{11}+k_{22}T^{\mathrm{N}}_{22}-2k_{12}T^{\mathrm{N}}_{12}+\frac{2M^{\mathrm{N}}_{11}}{A_1^2l_1^2}+\frac{2M^{\mathrm{N}}_{22}}{A_2^2l_2^2}\right)\omega\big|_{i,j}-M^{\mathrm{N}}_{11}\frac{\omega}{A_1^2l_1^2}\bigg|_{i+1,j}-M^{\mathrm{N}}_{11}\frac{\omega}{A_1^2l_1^2}\bigg|_{i-1,j}$$

$$-M^{\mathrm{N}}_{11}\frac{\partial A_1}{\partial\alpha_1}\frac{\omega}{A_1^3l_1}\bigg|^{i+1/2,\,j}_{i-1/2,\,j}-M^{\mathrm{N}}_{22}\frac{\omega}{A_2^2l_2^2}\bigg|_{i,j+1}-M^{\mathrm{N}}_{22}\frac{\omega}{A_2^2l_2^2}\bigg|_{i,j-1}-M^{\mathrm{N}}_{22}\frac{\partial A_2}{\partial\alpha_2}\frac{\omega}{A_2^3l_2}\bigg|^{i,\,j+1/2}_{i,\,j-1/2}$$

$$+2\left(-M^{\mathrm{N}}_{12}\frac{\omega}{A_1A_2l_1l_2}\bigg|^{i+1/2,\,j+1/2}_{i-1/2,\,j+1/2}+M^{\mathrm{N}}_{12}\frac{\omega}{A_1A_2l_1l_2}\bigg|^{i+1/2,\,j-1/2}_{i-1/2,\,j-1/2}-M^{\mathrm{N}}_{12}\frac{\partial A_1}{\partial\alpha_2}\frac{\omega}{A_1^2A_2l_1}\bigg|^{i+1/2,\,j}_{i-1/2,\,j}-M^{\mathrm{N}}_{12}\frac{\partial A_2}{\partial\alpha_1}\frac{\omega}{A_1A_2^2l_2}\bigg|^{i,\,j+1/2}_{i,\,j-1/2}\right)$$

$$-(T_{11}\varphi_1+T_{12}\varphi_2)\frac{\omega}{A_1l_1}\bigg|^{i+1/2,\,j}_{i-1/2,\,j}-(T_{22}\varphi_2+T_{12}\varphi_1)\frac{\omega}{A_2l_2}\bigg|^{i,\,j+1/2}_{i,\,j-1/2},\tag{2.11}$$

where $\omega=A_1A_2l_1l_2$.

This method for solving two-dimensional stress–strain problems for a shell with both nonlinearities has been implemented in a software package, which made it possible to obtain specific numerical results for cylindrical and conical shells with a circular hole [48, 62, 67], a spherical shell with an elliptic hole [66], and a spherical shell in the form of an eccentric ring [72].

2.3. Elastoplastic State of a Flexible Cylindrical Shell with a Circular Hole. We will present results from the stress–strain analysis [48] of a shell of radius R with a hole of radius ρ_0 subjected to internal pressure $p=\rho_0\cdot10^5$ Pa. The

TABLE 3

κ	θ	LP	GNP	PNP	PGNP
0.5	0	0.102	0.098	0.163	0.141
	$\pi/2$	0.113	0.115	0.184	0.152
1.0	0	0.130	0.132	0.391	0.291
	$\pi/2$	0.231	0.229	0.672	0.443
1.5	0	0.121	0.131	0.810	0.533
	$\pi/2$	0.592	0.680	1.294	0.939
2.0	0	0.242	—	1.015	0.632
	$\pi/2$	1.065	—	2.080	1.281

geometrical and mechanical parameters of the shell are $R = 56.25h$, $\rho_0 = (3.75 + 15)h$, $E = 67$ GPa, $v = 0.3$–0.5, $\sigma_n = 130$ MPa, $\varepsilon_n = 0.002$.

We choose a semigeodesic coordinate system (ρ, θ) for describing the midsurface of the shell and assume that the hole $(\rho = \rho_0)$ is closed by a special plug transmitting only the shearing forces $(Q_p = pp_0 / 2)$ to its boundary and that the stress state is a membrane one far from the perturbation zone $(\rho \ge \rho_n)$.

The linear and nonlinear problems have been solved for different geometrical parameters ($\kappa = \rho_0 / \sqrt{Rh} = 0.5$, 1.0, 1.5, 2.0) and different loads ($0 < p_0 > 20$). The data are given for $p_0 = 20$.

Table 3 collects the relative deflections (w / h) at two typical points $(\rho_0, 0)$ and $(\rho_0, \pi / 2)$ on the boundary of the hole for different geometrical parameters of the shell. The values have been found by solving linear, physically nonlinear, geometrically nonlinear, and physically and geometrically nonlinear problems.

Figures 4 and 5 show the variation of the maximum stresses ($\sigma_\theta = \sigma_\theta^0 \cdot 10^5$ Pa) along the boundary of the hole on the inside (case *a*) and outside (case *b*) surfaces of the shell (curves *1*, *2*, *3*, and *4* correspond to LP, GNP, PNP, and PGNP, respectively) for two sets of geometrical parameters: $\kappa = 1.5$ (Fig. 1) and $\kappa = 0.5$ (Fig. 2).

It can be seen that the stresses peak on the boundary of the hole at the point $(\rho_0, 0)$ on the inside surface of the shell. Allowing for the nonlinearities reduces the maximum stresses compared with the linear elastic solution. For example, this decrease is 34% in the GNP, 66% in the PNP, and 71% in the PGNP if $\kappa = 1.5$ and 1.4%, 44%, and 46%, respectively, if $\kappa = 0.5$.

3. Variational Difference Method. Algorithmic Implementation of the Kirchhoff–Love Hypotheses. The idea of this approach is to use Lagrangian multipliers to incorporate the Kirchhoff–Love constraints into the Timoshenko theory of shells. Unlike similar approaches, the Lagrangian multipliers are varied functions as the primary independent functions of the problem (displacements) are.

The idea was implemented in [8] and further developed in [13, 17, 18, 49, 50, 51, 52] in solving linear and nonlinear problems and related problems [61].

Variational principles and methods in the theory of shells are addressed in the monographs [1, 5].

In what follows, we will outline the key aspects of the algorithmic implementation of the Kirchhoff–Love constraints in the VDM (see [52] and the references therein for more details).

3.1. Basic Equations. Consider a thin orthotropic shell made of a nonlinear elastic composite. Its midsurface is described in a coordinate system $(\alpha_1, \alpha_2, \alpha_3)$ aligned with the lines of principal curvature.

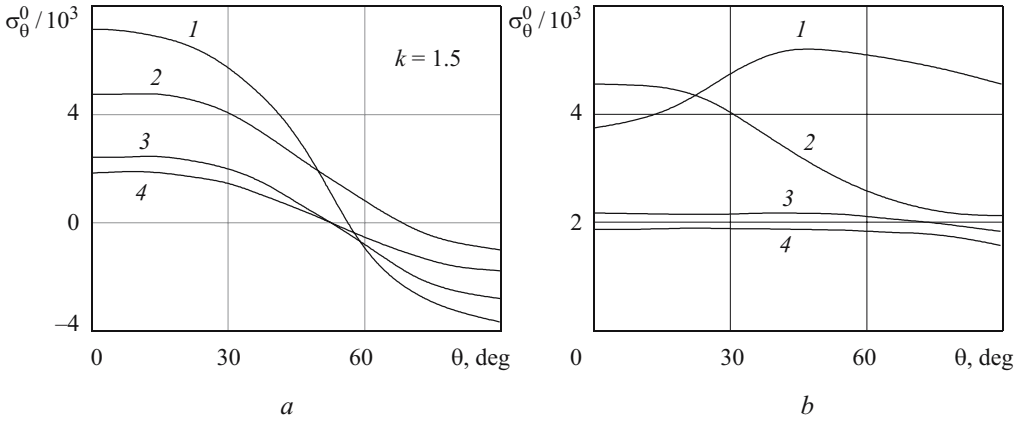

Fig. 4

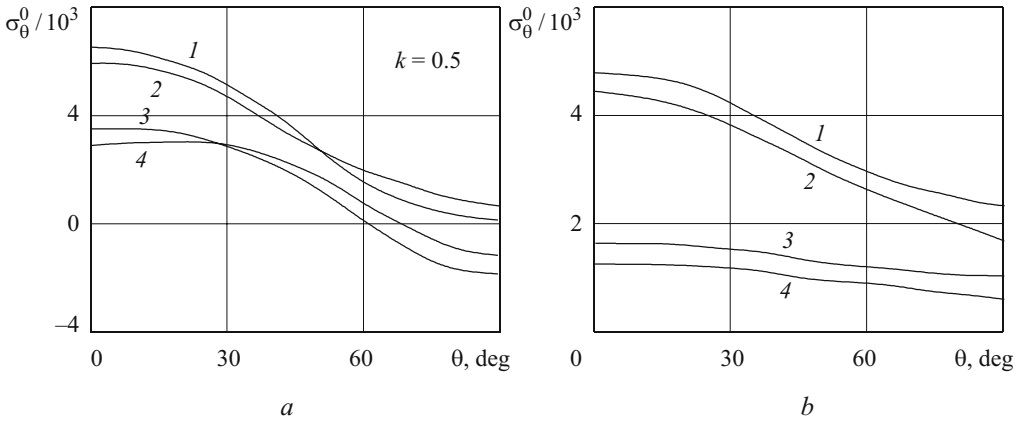

Fig. 5

Note that the static part ($\sigma_{33} = 0$) of the hypotheses that the normal stresses are small is the same in the cases of the Kirchhoff–Love and Timoshenko hypotheses. Formally the same formulas express the displacement components of an arbitrary point of the shell in terms of the displacements u_1, u_2, and u_3 of its midsurface and the angles of rotation φ_1 and φ_2 of the normal:

$$U_1(\alpha_1, \alpha_2, \alpha_3) = u_1(\alpha_1, \alpha_2) + \alpha_3 \varphi_1(\alpha_1, \alpha_2),\ U_2(\alpha_1, \alpha_2, \alpha_3) = u_2(\alpha_1, \alpha_2) + \alpha_3 \varphi_2(\alpha_1, \alpha_2),$$

$$U_3(\alpha_1, \alpha_2, \alpha_3) = u_3(\alpha_1, \alpha_2).$$

The difference is in that φ_1 and φ_2 are independent functions in the case of the Timoshenko hypotheses and are determined by equating the transverse-shear strains to zero,

$$\varepsilon_{13} = \varepsilon_{23} = 0, \tag{3.1}$$

and equal to the angles of rotation of tangents in the case of the Kirchhoff–Love hypotheses.

This circumstance allows us to derive a functional for thin shells from the functional for shells subject to transverse shears. With geometrically linear and physically nonlinear relations, the mixed functional has the form

$$\prod(u_1, u_2, u_3, \varphi_1, \varphi_2, T_{13}^f, T_{23}^f)$$

$$= \iint_\Omega A(u_1, u_2, u_3, \varphi_1, \varphi_2) d\Omega - A_n - A_k + \iint_\Omega (T_{13}^f \varepsilon_{13} + T_{23}^f \varepsilon_{23}) d\Omega, \tag{3.2}$$

where $\{U\} = \{u_1, u_2, u_3, \varphi_1, \varphi_2, T_{13}^f, T_{23}^f\}$ is the vector of unknown functions; A_n and A_k are the works done by the external surface and boundary forces; A is the strain energy density,

$$\delta A = T_{11}\delta\varepsilon_{11} + T_{22}\delta\varepsilon_{22} + T_{12}\delta\varepsilon_{12} + M_{11}\delta\kappa_{11} + M_{22}\delta\kappa_{22} + 2M_{12}\delta\kappa_{12}.$$

In (3.2), the Kirchhoff–Love kinematics (3.1) is implemented algorithmically, using Lagrangian multipliers (T_{13}^f, T_{23}^f), which are shearing forces. The superscript "*f*" in (3.2) indicates that the function is varied, unlike, for example, the shear strains, which are expressed as

$$\varepsilon_{13} = \varphi_1 + \frac{1}{A_1}\frac{\partial u_3}{\partial \alpha_1} - k_1 u_1 \quad (1 \leftrightarrow 2),$$

where $A_i\,(i = 1, 2)$ are the coefficients of the first quadratic form; k_i are the curvatures of the midsurface.

Since the shearing forces T_{13}^f and T_{23}^f are assumed independent functions, they can be set, as displacements, before constructing a functional, on that portion of the shell boundary where they are known. For instance, it is expedient to set $T_{i3}^f = 0$ on the lines of symmetry $\alpha_i = \text{const}$ because $\varepsilon_{i3} = 0$ always there.

If the stress state is plane, the constitutive equations are

$$e_{11} = \left(\frac{1}{E_{11}} + \Psi q_{1111}\right)\sigma_{11} + \left(-\frac{\nu_{12}}{E_{22}} + \Psi q_{1122}\right)\sigma_{22} \quad (1 \leftrightarrow 2),$$

$$e_{12} = \left(\frac{1}{G_{12}} + 4\Psi q_{1212}\right)\sigma_{12}, \tag{3.3}$$

where E_{11}, E_{22}, G_{12}, and ν_{12} are the elastic constants of the composite; $\Psi(f)$ is a function describing the nonlinear deformation of an orthotropic material; $q_{1111}, q_{2222}, q_{1122}$, and q_{1212} are the components of a tensor that accounts for the anisotropy of the composite; and *f* is the quadratic stress function [13, 16].

3.2. Methodical Aspects of Numerical Solution of Nonlinear Problems. The procedure is based on the MSA and VDM and outlined in [49, 50]. Use is made of the Lagrange equation $\delta\Pi = 0$ and Eqs. (3.1)–(3.3). It is assumed that nonlinear parts in the basic equations are known from the previous approximation and not varied. Finally, we arrive at a system of algebraic equations [50], which can be briefly represented at the point (i, j) as

$$\sum_{k=i-1}^{i+1}\sum_{l=j-1}^{j+1}\sum_{n=1}^{K^F} A_{mn}(k,l) f_n(k,l) = \Delta V(i,j) q_m(i,j) + \Delta s(i,j) T_{\nu m}(i,j) + \Phi_m(i,j),$$

$$m = \overline{1, K^F}, \quad i = \overline{1, K^I}, \quad j = \overline{1, K^J}, \tag{3.4}$$

where $[A]$ is a symmetric band matrix of variable coefficients; $\{\Phi\}$ is the vector of nonlinear terms; $\{q\}$ and $\{T_\nu\}$ are the vectors of surface and boundary loads; ΔV and Δs are the discrete analogs of surface and arc elements; K^I and K^J are the number of nodes of the mesh along the α_1- and α_2-axes, respectively.

Note that if the functional is mixed, negative numbers may appear on the diagonal. The system is solved by the Cholesky square-root method as more stable. For $\sqrt{-1}$ not to appear on the diagonal, the equation is algorithmically divided by $\sqrt{-1}$. Though the stability theorems for the Cholesky method are proved for positive definite matrices, experience suggests that the method also works in the case being considered.

To calculate the nonlinear terms $\{\Phi\}$ in (3.4), it is necessary to resolve the nonlinear constitutive equations (3.3) for the stresses. We represent them in the form

$$F_i(\{\sigma\}, \{e\}) = 0 \quad (i = \overline{1, 3}), \tag{3.5}$$

where $\{\sigma\} = \{\sigma_{11}, \sigma_{22}, \sigma_{12}\}^{\mathrm{T}}$ and $\{e\} = \{e_{11}, e_{22}, e_{12}\}^{\mathrm{T}}$. The nonlinear system of equations (3.5) is numerically solved by Newton's method:

$$\{\sigma^{j+1}\} = \{\sigma^{j}\} + \{\Delta\sigma^{j}\}, \tag{3.6}$$

where the increments $\{\Delta\sigma^{j}\}$ at the jth step are found by solving the linear algebraic system of equations

$$F_i + \frac{\partial F_i}{\partial\{\sigma^{j}\}}\{\Delta\sigma^{j}\} = 0, \tag{3.7}$$

using the stress $\{\sigma^{1}\} = \{\sigma^{0}\}$ for a linear elastic body as the initial approximation. The iterative process (3.5)–(3.7) is terminated once the maximum (in absolute magnitude) stress components in two successive iterations differ by less than a predefined tolerance. The same method was used for the numerical inversion of the nonlinear constitutive equations (1.3) in axisymmetric problems based on the FDM.

Thus, the nonlinear elastic deformation of a shell can be analyzed by solving a sequence of Eqs. (3.4) with appropriate boundary conditions. The algorithm for the numerical solution of nonlinear problems and the software for the stress–strain analysis of shells allow us to calculate the displacements, angles of rotation, shearing forces $\{U\}$, and strain and stress tensors taking into account the varying parameters of the shell, level and type of load, the properties of the material, and the type of boundary conditions.

Numerous examples of solving nonlinear, linear, so-called pathological [57] test problems are given in [52].

Noteworthy is the positive experience of [8, 18] in using Lagrangian multipliers to implement the kinematic hypotheses of the theory of thin shells in solving linear and nonlinear problems by the VDM. Though the computational effort has somewhat increased and the matrix of the system of algebraic equations resulting from the application of the VDM and MSA is no longer positive definite, we have got a more algorithmic approach to both derivation and numerical solution of the governing equations. For physically nonlinear problems, there is no need to perform calculations for the shearing forces T_{13}^{f} and T_{23}^{f} because they, actually, are Lagrangian multipliers and determined automatically. Geometrically nonlinear problems can be simplified for thin shells subject to considerable bending because there is no need to explicitly express the angles of rotation of the normal in terms of the displacements.

4. Finite-Element Method. In the theory of thin shells based on the Kirchhoff–Love hypotheses, the solution must satisfy severe smoothness conditions. This means that when problems for thin shells are solved by the finite-element method, approximating functions for the displacement components should be selected so that the tangential displacements u and v are continuous functions, and the deflection w is continuous together with its first derivatives on the sides of a finite element [9, 22]. Practically, deriving piecewise-continuous polynomial expressions with continuous first derivatives involves certain difficulties. A number of finite elements [9, 22, 38] that satisfy compatibility conditions have been developed. We will consider two types of finite elements for design of thin shells: traditional (classical) and modified.

In exposing the principles of the finite-element method, it is convenient to represent the equations of the theory of shells in matrix form.

4.1. Matrix Equations of the Theory of Shells. The nonlinear kinematic equations for thin shells in a curvilinear orthogonal coordinate system $(\alpha_1, \alpha_2, \gamma)$ not aligned with the lines of principal curvature have the following matrix form [44]:

$$\{\Im\} = \{\varepsilon_{11}, \varepsilon_{22}, \varepsilon_{12}, \kappa_{11}, \kappa_{22}, 2\kappa_{12}\}^{\mathrm{T}} = \{\{\varepsilon\}^{\mathrm{T}}, \{\kappa\}^{\mathrm{T}}\}^{\mathrm{T}} = \{\Im^{0}\} + \{\Im^{\mathrm{N}}\},$$

$$\{\varepsilon\} = \{\varepsilon_{11}, \varepsilon_{22}, \varepsilon_{12}\}^{\mathrm{T}} = \{\varepsilon^{0}\} + \{\varepsilon^{\mathrm{N}}\} = [A_{\varepsilon}]\{U\} + \frac{1}{2}[A_{L}]\{\varphi\},$$

$$\{\kappa\} = \{\kappa_{11}, \kappa_{22}, 2\kappa_{12}\}^{\mathrm{T}} = \{\kappa^{0}\} = [A_{æ}]\{\varphi\}, \qquad \{\varphi\} = [A_{\varphi}]\{U\},$$

$$\{e\} = \{e_{11}, e_{22}, e_{12}\}^{\mathrm{T}} = \{\varepsilon\} + \gamma\{\kappa\} = \{e^{0}\} + \{e^{\mathrm{N}}\},$$

$$\{e^{0}\} = \{\varepsilon^{0}\} + \gamma\{\kappa\}, \qquad \{e^{\mathrm{N}}\} = \{\varepsilon^{\mathrm{N}}\}, \tag{4.1}$$

where ε_{ij} and κ_{ij} are the membrane and bending strains of the shell's midsurface; $\{U\} = \{u, v, w\}^{\mathrm{T}}$ and $\{\varphi\} = \{\varphi_1, \varphi_2\}^{\mathrm{T}}$ are the vector of displacements and the angles of rotation; $[A_\varepsilon]$, $[A_\kappa]$, and $[A_\varphi]$ are the matrices of linear differentiation operations; and $[A_{\mathrm{L}}]$ is the matrix of angles of rotation.

To analyze the elastoplastic stress–strain state of a shell under complex loading, we will use the theory of flow with isotropic hardening that employs the Mises yield criterion and the associated flow rule [12]. Let the total strain $\{e\}$ consist of elastic $\{e^{\mathrm{el}}\}$ and plastic $\{e^{\mathrm{pl}}\}$ components. Then the stress vector $\{\sigma\} = \{\sigma_{11}, \sigma_{22}, \sigma_{12}\}^{\mathrm{T}}$ depends on the strain vector $\{e\}$ as follows:

$$\{\sigma\} = [D](\{e\} - \{e^{\mathrm{pl}}\}) = [D]\{e\} + \{\sigma^{\mathrm{pl}}\} = [D]\{e^0\} + \{\sigma^{\mathrm{N}}\}, \tag{4.2}$$

where $\{\sigma^{\mathrm{pl}}\} = -[D\{e^{\mathrm{pl}}\}$, $\{\sigma^{\mathrm{N}}\} = [D]\{e^{\mathrm{N}}\} + \{\sigma^{\mathrm{pl}}\}$, $[D]$ is the stiffness matrix for a plane stress state.

Considering Eqs. (4.1) and (4.2), we represent the vector of internal forces (T_{ij}) and moments (M_{ij}) as the sum of linear and nonlinear terms [12]:

$$\{m\} = \{T_{11}, T_{22}, T_{12}, M_{11}, M_{22} M_{12}\}^{\mathrm{T}} = \{\{T\}^{\mathrm{T}}, \{M\}^{\mathrm{T}}\}^{\mathrm{T}},$$

$$\{m\} = \{m^{\mathrm{el}}\} + \{m^{\mathrm{pl}}\} = \{m^0\} + \{m^{\mathrm{N}}\}, \tag{4.3}$$

where $\{m^0\} = \{T_{11}^0, T_{22}^0, T_{12}^0, M_{11}^0, M_{22}^0, M_{12}^0\}^{\mathrm{T}}$ $(0 \to y, p, H)$, $[D^0]$ is the stiffness matrix of the shell; $\{m^0\} = [D^0]\{\Im^0\}$ correspond to the linear elastic case, $\{m^{\mathrm{el}}\} = [D^0]\{\Im\}$ to the geometrically nonlinear case; $\{m^{\mathrm{pl}}\}$ to the physically nonlinear case, and $\{m^{\mathrm{N}}\}$ to the physically and geometrically nonlinear case.

4.2. Finite-Element Method for Solving Nonlinear Problems for Shells. Considering the essential nonlinearity of (4.1), (4.2), and (4.3) and seeking to trace the deformation history of the shell, we use the procedure of incremental loading and represent the original equations in incremental form to derive the governing equations. To this end, we also use the virtual-displacement principle [1, 5], the modified Newton–Kantorovich method, the method of additional stresses, and the finite-element method.

Applying the procedure of incremental loading and performing linearization, we arrive at the following functional [44]:

$$\Pi = \frac{1}{2}\iint\limits_{(\Sigma)} (\{\Delta\Im^{\mathrm{L}}\}^{\mathrm{T}}[D^0]\{\Delta\Im^{\mathrm{L}}\} + \{\Delta\varphi\}^{\mathrm{T}}[\Delta A_L]^{\mathrm{T}}\{\overline{T}\})d\Sigma + \iint\limits_{(\Sigma)} (\{\Delta\Im^{\mathrm{L}}\}^{\mathrm{T}}\{\Delta m^{\mathrm{N}}\} + \{\Delta\varphi\}^{\mathrm{T}}[\Delta A_L]^{\mathrm{T}}\{\Delta T\})d\Sigma$$

$$-\iint\limits_{(\Sigma)} \{\Delta U\}^{\mathrm{T}}\{\Delta p\}d\Sigma - \int\limits_{(\Gamma_k)} \{\Delta U_k\}^{\mathrm{T}}\{\Delta m_k\}ds + \iint\limits_{(\Sigma)} (\{\Delta\Im^{\mathrm{L}}\}^{\mathrm{T}}\{\overline{m}\} - \{\Delta U\}^{\mathrm{T}}\{\overline{p}\})d\Sigma - \int\limits_{(\Gamma_k)} \{\Delta U_k\}\{\overline{m}_k\}ds, \tag{4.4}$$

where $\{\overline{T}\}$, $\{\overline{m}\}$, $\{\overline{p}\}$, $\{\overline{m}_k\}$ and $\{\Delta T\}$, $\{\Delta m\}$, $\{\Delta p\}$, $\{\Delta m_k\}$ are the components of the vectors of internal mechanical factors, surface load, and boundary forces at the beginning of the ith step, and their increments at this step; $\{\Delta m^{\mathrm{N}}\}$ is the vector of increments of nonlinear forces and moments; $\{\Delta\varphi\}$, $\{\Delta U\}$, $\{\Delta U_k\}$, and $\{\Delta\Im^{\mathrm{L}}\}$ are the increments of the angles of rotation, displacements of the midsurface and boundary of the shell, and linearized strains at the ith step; Σ_p is the portion of the midsurface (Σ) on which a surface load is prescribed; and Γ_k is the portion of the boundary (Γ) on which boundary forces are prescribed.

In solving two-dimensional linear boundary-value problems, we use the finite-element method in each of the successive approximations. To this end, the midsurface (Σ) is partitioned into E finite elements, within each of which the components of the vector of displacement increments $\{\Delta U\}$ are represented as polynomials of two variables [9, 22]:

$$\{\Delta U\} = [f^{(\mathrm{e})}]\{\Delta q^{(\mathrm{e})}\}, \tag{4.5}$$

where $\{\Delta q^{(\mathrm{e})}\} = \{\Delta q_1, \Delta q_2, \ldots, \Delta q_n\}^{\mathrm{T}}$ is the column vector of increments of degrees of freedom of an element (e); $f^{(\mathrm{e})}$ is the $3 \times n$ matrix of the shape function. Using formulas (4.1) and (4.5), we derive expressions for the increments of the strain components.

The stationarity conditions for the discrete analog of the linearized functional (4.4) yield a system of governing algebraic equations, which has the following matrix form at the ith step of loading [44]:

$$\left([K_0]+[K_\varphi]+[K_\sigma]\right)\{\Delta q\}=\{\Delta P\}-\{\Delta\Omega\}+\{\Delta\Psi\}, \tag{4.6}$$

where $[K_0]$ is the stiffness matrix of a linear elastic shell; $[K_\varphi]$ and $[K_\sigma]$ are the influence matrices of initial angles of rotation and stresses; $\{\Delta q\}$ is the vector of increments of nodal degrees of freedom; $\{\Delta P\}$ is the load vector; $\{\Delta\Omega\}$ is the vector of nonlinearities; and $\{\Delta\Psi\}$ is the vector of residuals of the equilibrium equations at the end of the $(i-1)$th step of loading.

To solve specific boundary-value problems, the governing equations (4.6) should be supplemented with appropriate boundary conditions at the edges of the shell and the boundaries of the holes. They can be prescribed for displacements, forces, or in mixed form.

4.3. Classical Finite Element for Thin Shells of Simple Geometry (Analytic Implementation of the Kirchhoff–Love Hypotheses). Let us outline the principles of the FEM applied to solve nonlinear problems for shells with holes. If the domain (Σ) of variation in the curvilinear coordinates (α_1,α_2) is not canonical (rectangular), the midsurface of the shell is parametrized. We will consider two cases of parametrization.

For doubly connected domains (Σ) bounded by two smooth curves (Γ_1,Γ_2) that do not intersect and do not touch each other, the following equation is used for parametrization [44]:

$$\vec{r}=\vec{r}_\phi+F(r,\theta)\vec{e}_\phi, \tag{4.7}$$

where r and θ are the parametrization variables; $\vec{r}$ and $\vec{r}_\phi$ are the position vectors of the points $M\in(\Sigma)$ and $M_\phi\in(\Sigma_\phi)$, respectively; (Σ_ϕ) is a ring $(r_n\le r\le r_k,\ 0\le\theta\le 2\pi)$ on the midsurface that is mapped by Eq. (4.7) onto the domain (Σ); $\vec{e}_\phi$ is the unit vector of the coordinate line $\theta=\text{const}$; and $F(r,\theta)$ is a function such that $F(r,\theta)=A(\theta)+rB(\theta)$.

In the more general case of a noncanonical domain (Σ) bounded by four smooth curves, the following compound function is used for parametrization [10]:

$$\vec{r}_k(\beta_1,\beta_2)=-\varphi(\beta_1)\vec{F}(\beta_1,\beta_2)\varphi(\beta_2)\quad(-1\le\beta_1\le 1),$$

$$\varphi(\beta_1)=\{-1,\varphi_1(\beta_1),\varphi_2(\beta_1)\},\quad \varphi_1(\beta_1)=0.5(1-\beta_1),$$

$$\varphi_2(\beta_1)=0.5(1+\beta_1)\quad(\beta_1\to\beta_2), \tag{4.8}$$

where $\vec{F}(\beta_1,\beta_2)$ is a 3×3 matrix whose elements are the position vectors of the boundaries and nodes of the domain (Σ).

The domain of parametrization coordinates is a rectangle or square (Σ_s). Let us cover the domain (Σ_s) with a mesh of rectangular finite elements (FEs) whose sides are parallel to the parametrization lines.

Within each FE, the tangential displacements are approximated by bilinear functions, and the deflections by bicubic splines [9, 22]:

$$u=\sum_{i=1}^{4}u^{(i)}N_i(\xi_1,\xi_2),\qquad v=\sum_{i=1}^{4}v^{(i)}N_i(\xi_1,\xi_2),$$

$$w=\sum_{i=1}^{4}[w^{(i)}N_i^{(1)}(\xi_1,\xi_2)+w_{\beta_1}^{(i)}N_i^{(2)}(\xi_1,\xi_2)+w_{\beta_2}^{(i)}N_i^{(3)}(\xi_1,\xi_2)+w_{\beta_1\beta_2}^{(i)}N_i^{(4)}(\xi_1,\xi_2)], \tag{4.9}$$

where $u^{(i)},v^{(i)},w^{(i)},w_{\beta_1}^{(i)},w_{\beta_2}^{(i)}$, and $w_{\beta_1\beta_2}^{(i)}$ are the nodal displacements and derivatives of the deflection at the ith node; $N_i(\xi_1,\xi_2)$ and $N_i^{(j)}(\xi_1,\xi_2)$ are the shape functions as a product of one-dimensional Hermite polynomials of the local coordinates ξ_1 and ξ_2.

The partial derivatives of the shape functions with respect to α_1 and α_2 in the expressions for the strain components are evaluated using the formulas for the differentiation of a complex function of several variables.

The finite element (4.9) satisfies the continuity conditions for the first derivative of the deflection and has 24 degrees of freedom (six at each node). Note that the main shortcoming of this element is the unsatisfactory approximation of its rigid-body displacements.

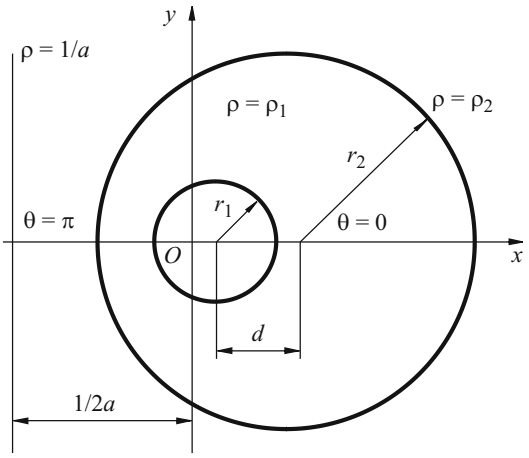

Fig. 6

Let us also present the relations for the finite element proposed in [3]. It uses identical bicubic approximations of all the three displacements:

$$u=\sum_{i=1}^{4}[u^{(i)}N_i^{(1)}(\xi_1,\xi_2)+u_{\beta_1}^{(i)}N_i^{(2)}(\xi_1,\xi_2)+u_{\beta_2}^{(i)}N_i^{(3)}(\xi_1,\xi_2)+u_{\beta_1\beta_2}^{(i)}N_i^{(4)}(\xi_1,\xi_2)]\quad(u\to v),$$

$$w=\sum_{i=1}^{4}[w^{(i)}N_i^{(1)}(\xi_1,\xi_2)+w_{\beta_1}^{(i)}N_i^{(2)}(\xi_1,\xi_2)+w_{\beta_2}^{(i)}N_i^{(3)}(\xi_1,\xi_2)+w_{\beta_1\beta_2}^{(i)}N_i^{(4)}(\xi_1,\xi_2)]. \tag{4.10}$$

The finite element (4.10) has 48 degrees of freedom, satisfies the compatibility conditions, and quite accurately approximates the rigid-body displacements.

4.4. Modified Finite Element for Thin Shells of Complex Geometry (Discrete Implementation of the Kirchhoff–Love Hypotheses). If the domain of parametrization coordinates is complex (noncanonical), it cannot be partitioned into only rectangular elements. To design shells of such geometry, use is made of elements with sides nonaligned with the parametrization lines. Constructing a FE in this case involves certain difficulties associated with the selection of approximating functions for the deflection that would satisfy the continuity conditions for the first derivatives.

A modified FE for thin shells of complex geometry that satisfies the continuity conditions was proposed in [44]. A feature of this FE is that the angles of rotation φ_1 and φ_2 in the expressions for the flexural strains are not defined by (4.1), as is the case in the classical FEM, and are approximated by biquadratic serendipity polynomials [9], with the geometrical Kirchhoff–Love hypotheses being valid only at the FE nodes. Such an approach is, in essence, the use of discrete Kirchhoff–Love constraints. A method for the discrete implementation of the Kirchhoff–Love hypotheses was first proposed in [45, 70]. The angle of rotation of the normal about the tangent to the boundary of the FE is assumed to vary linearly along the side of the FE. The membrane strains are calculated using vector expressions for strains and approximating the displacement vector $\vec{U}$ on the axes of the global Cartesian coordinate system (X, Y, Z):

$$\varepsilon_{11}=\frac{\partial\vec{U}}{A_1\partial\alpha_1}\cdot\vec{e}_1+\frac{1}{2}\left(\frac{\partial\vec{U}}{A_1\partial\alpha_1}\cdot\vec{n}\right)^2\quad(1\to 2),$$

$$\varepsilon_{12}=\frac{\partial\vec{U}}{A_1\partial\alpha_1}\cdot\vec{e}_2+\frac{\partial\vec{U}}{A_2\partial\alpha_2}\cdot\vec{e}_1+\left(\frac{\partial\vec{U}}{A_1\partial\alpha_1}\cdot\vec{n}\right)\left(\frac{\partial\vec{U}}{A_2\partial\alpha_2}\cdot\vec{n}\right), \tag{4.11}$$

where $\vec{e}_1$, $\vec{e}_2$, and $\vec{n}$ are the unit vectors of the coordinate system $(\alpha_1, \alpha_2, \gamma)$.

In determining the membrane strains this way, it is possible to make accurate allowance for the rigid-body translation of the FE.

TABLE 4

d/r	θ	ξ	σ_θ^0		$e_\theta \cdot 10^2$		w/h	
			LP	PGNP	LP	PGNP	LP	PGNP
4.5	0	0.5	5265	1853	0.7610	1.2020	1.561	1.825
		–0.5	3430	1769	0.4985	0.8264		
	π	0.5	3446	1658	0.4979	0.7607	1.071	1.273
		–0.5	2551	1501	0.3693	0.4758		
4.0	0	0.5	5114	1882	0.7392	1.1600	1.592	1.831
		–0.5	3116	1826	0.4526	0.7965		
	π	0.5	5421	1806	0.7827	1.1090	1.776	1.818
		–0.5	2958	1690	0.4297	0.7185		
3.0	0	0.5	5010	1958	0.7233	1.1220	1.579	1.828
		–0.5	3049	1929	0.4407	0.7693		
	π	0.5	5235	1858	0.7549	1.1750	1.710	1.943
		–0.5	3136	1805	0.4521	0.7928		
0.0	0	0.5	5141	1891	0.7367	1.1630	1.674	1.941
		–0.5	2961	1806	0.4241	0.7719		

This FE satisfies the continuity conditions for the angles of rotation on its sides, has 20 degrees of freedom, and is used to design both shells of simple geometry and shells whose midsurface boundary contains more than four corner points.

Note that this approach and algorithm allow us to obtain, as special cases, the solutions of the elastoplastic (method of elastic solutions) and geometrically nonlinear (simple iteration method) problems. Comparative analyses of the solutions of linear and nonlinear axisymmetric problems for shells of revolution and two-dimensional stress-concentration problems for shells with one or two holes lead us to conclude that our approach is efficient and can be used to solve doubly nonlinear problems for shells of complex geometry.

4.5. Inelastic Deformation of a Flexible Spherical Shell in the Form of an Eccentric Ring. Let us discuss the results from the stress–strain analysis [23] of a spherical shell of radius R and thickness h having the form of an eccentric ring in plan and being subjected to an internal pressure $p = 4 \cdot 10^5$ Pa. We denote the radii of the inside (circular hole) and outside boundaries of the shell by r_1 and r_2, respectively, and the distance between their centers by d (Fig. 6).

We will describe the midsurface of the shell using orthogonal curvilinear coordinates (ρ, θ) related to the Cartesian coordinates (x, y) by

$$x = \rho \frac{\cos\theta - a\rho}{1 - 2a\rho\cos\theta + a^2\rho^2}, \qquad y = \frac{\rho\sin\theta}{1 - 2a\rho\cos\theta + a^2\rho^2}. \tag{4.12}$$

The curves $\rho = \text{const}$ and $\theta = \text{const}$ are two orthogonal families of circles with the lines of centers lying on the x- and y-axes, respectively.

TABLE 5

d/r	ξ	σ_θ^0		σ_ρ^0		$e_\rho \cdot 10^2$	
		LP	PGNP	LP	PGNP	LP	PGNP
4.5	0.5	–1320	–1097	–4399	–2225	–0.5718	–1.3310
	–0.5	1642	1135	5475	2295	0.7117	1.6540
4.0	0.5	–295	–590	–983	–1679	–0.1278	–0.2756
	–0.5	703	859	2344	1964	0.3048	0.5261
3.0	0.5	–116	–189	–387	–631	–0.0504	–0.0820
	–0.5	484	540	1612	1633	0.2095	0.2435
0.0	0.5	–190	–186	–633	–622	–0.0822	–0.0809
	–0.5	543	532	1811	1626	0.2354	0.2390

The inside and outside boundaries of the shell coincide with the coordinate lines $\rho = \rho_1$ and $\rho = \rho_2$, respectively. The parameter a and the coordinates of the shell boundaries are defined by

$$a = d / \sqrt{(r_2^2 - r_1^2)^2 - 2d^2 (r_1^2 + r_2^2) + d^4},$$

$$\rho_1 = \frac{\sqrt{1 + 4r_1^2 a^2} - 1}{2r_1 a^2}, \quad \rho_2 = \frac{\sqrt{1 + 4r_2^2 a^2} - 1}{2r_2 a^2}. \tag{4.13}$$

The shell is made of AMg-6 alloy and has the following geometrical and mechanical characteristics: $R / h = 400$, $r_1 / h = 30$, $r_2 / r_1 = 6$, $d / r_1 = 0, 3, 4, 4.5$, $E = 70$ GPa, $\nu = 0.3$–0.5, $\sigma_n = 140$ MPa, $\varepsilon_n = 0.002$.

The hole is assumed to be closed with a special plug that transmits only the shearing forces $Q_к = qr_1 / 2$ to the inside boundary. The outside boundary is clamped.

For reasons of geometrical and mechanical symmetry, the problem can be solved in the domain ($\rho_1 \le \rho \le \rho_2$, $0 \le \theta \le \pi$) covered with a uniform 16×16 FE mesh.

Table 4 summarizes the stresses ($\sigma_\theta = \sigma_\theta^0 \cdot 10^5$ Pa), strains (ε_θ), and relative deflections (w / h) at two points ($\rho = \rho_1$, $\theta = 0$) and ($\rho = \rho_1$, $\theta = \pi$) of the hole boundary on different surfaces ($\xi = \pm 0.5$) for both LPs and PGNPs and the following distances between the centers of the outside and inside boundaries: $d/r_1 = 0, 3, 4, 4.5$.

The stresses ($\sigma_\theta^0, \sigma_\rho^0$) and strains ($\varepsilon_\rho$) at the point ($\rho = \rho_2$, $\theta = \pi$) of the outside boundary on different surfaces are given in Table 5.

It can be seen that the hoop stresses (σ_θ), strains (ε_θ), and deflections (w) simultaneously peak on the hole boundary at the point ($\rho = \rho_1$, $\theta = \pi$) in the LP for $d/r_1 = 3, 4$ and at the point ($\rho = \rho_1$, $\theta = 0$) in the PGNP for $d / r_1 = 4$. The section at these points on the outside surface of the shell is most critical.

The closer the shell boundaries, the less stressed the free boundary and the higher the stress concentration on the clamped boundary.

When both plastic strains and finite deflections are allowed for, the stresses level off throughout the thickness of the shell and along the boundary of the hole and the maximum stresses decrease, compared with the linear elastic solution, by 63, 64, 67, 58%, and the maximum deflections increase by 14, 12, 2, 14%, and the maximum strains increase by 37, 36, 33, 54% for $d/r_1 = 0, 3, 4, 4.5$, respectively.

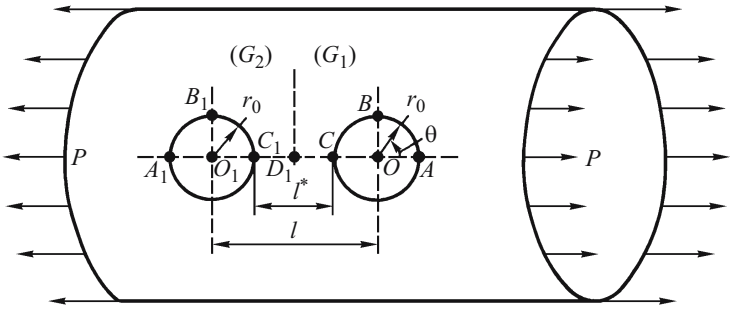

Fig. 7

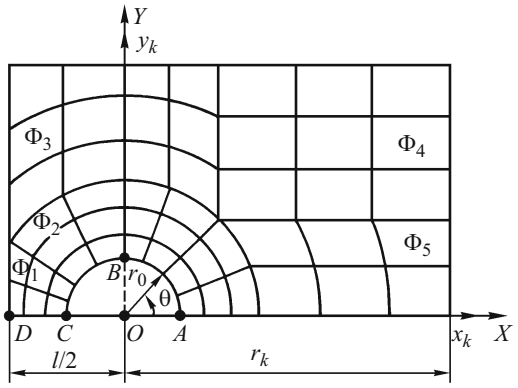

Fig. 8

4.6. Elastoplastic Deformation of a Flexible Cylindrical Shell with Two Circular Holes. Numerical solutions of physically and geometrically nonlinear stress–strain problems for a cylindrical shell with two circular holes are presented in [63, 65]. We will analyze the elastoplastic state of a thin-walled cylindrical shell with two equal circular holes with centers on one generatrix (Fig. 7). The shell is under axial tensile forces P ($P / h = P_0 / h \cdot 10^5$ Pa).

The shell has the following geometrical and mechanical parameters [63]:

$$\tilde{r} = r_0 / \sqrt{Rh} = 2, \quad \tilde{l} = l / r_0 = 2, 3, \ldots, 4 \ (l^*/r_0 = 0.3\text{–}2.0), \quad E = 0.65 \text{ GPa},$$

$$\nu = 0.3\text{–}0.5, \quad \sigma_n = 130 \text{ MPa}, \quad \varepsilon_{\text{П}} = 0.002, \quad \sigma_{\text{т}} = 165 \text{ MPa}, \quad \sigma_{\text{в}} = 325 \text{ MPa}, \tag{4.14}$$

where R and h are the radius and thickness of the shell; $r_0 = r_1 = r_2$ is the radius of the holes; $\tilde{l}\,(l^*)$ is the distance between the centers (boundaries) of the holes.

The shell is described in a Cartesian coordinate system (x, y, z); (r, θ) is a polar coordinate system with the pole at the center of the hole.

The boundaries of the holes are assumed to be free from reinforcements and forces ($T_k = S_k = Q_k = 0, M_k = 0$), and the stress state is membrane far from the holes:

$$\text{on the boundary } x = x_k: \qquad \tilde{T}_{xy} = \tilde{Q}_x^* = 0, \quad M_x = 0, \quad \tilde{T}_x = P, \tag{4.15}$$

$$\text{on the boundary } y = y_k: \qquad \tilde{T}_y = \tilde{T}_{xy} = 0, \quad M_y = 0, \quad w = -\nu PR / Eh. \tag{4.16}$$

Symmetry conditions hold on the lines $y = 0$ and $x = l/2$ (Fig. 8).

Given (4.14), (4.15), (4.16), and load ($P_0 = 1300h$), the loading process was divided into 10 steps. For reasons of mechanical and geometrical symmetry, just a quarter the midsurface was considered. This domain was divided into fragments Φ_i ($i = \overline{1,4}$), each partitioned into quadrangular FEs.

Table 6 summarizes the maximum hoop stresses ($\sigma_\theta = \sigma_\theta^0 \cdot 10^5$ Pa) along the boundary of the hole at three points throughout the thickness ($\xi = z / h = 0, \pm 0.5$) for $\tilde{l} = 2.3, 2.5, 3.0, 4.0$. These results have been obtained by solving LP, PNP, GNP, and PGNP.

Table 7 gives the radial and hoop stresses ($\sigma_i = \sigma_i^0 \cdot 10^5$ Pa, $i = r, \theta$) at the center of the bridge (point D) on the outside and inside surfaces ($\xi = \pm 0.5$).

It can be seen that the stresses change insignificantly on the boundary segment ($0 \le \theta \le \pi / 2$). The interaction of the holes can be neglected at the point A ($r = r_0, \theta = 0$), which is the farthest from the second hole. The change in the stresses at the point C ($r = r_0, \theta = \pi$), which is closest to the second hole, is insignificant compared with shells under internal pressure [65]. Thus, when a shell (even with closely spaced holes $\tilde{l} = 2, 3$) is subject to axial tensile forces, the point (B) in the section ($r = r_0, \theta = \pi / 2$) on the inside surface ($\xi = -0.5$) is the most critical.

TABLE 6

$\tilde{l}$	θ	ξ	σ_θ^0			
			LP	PNP	GNP	PGNP
2.3	0	0.5	299	1300	1044	1687
		–0.5	–2582	–1737	–2284	–1676
	π/2	0.5	3952	1997	4209	2059
		–0.5	6037	2457	4430	2069
	π	0.5	1603	1821	1577	1748
		–0.5	–2151	–1894	–1595	–1620
2.5	0	0.5	290	1266	995	1664
		–0.5	–2577	–1738	–2252	–1674
	π/2	0.5	3963	2011	4224	2071
		–0.5	6062	2473	4433	2080
	π	0.5	1345	1723	1263	1600
		–0.5	–1589	–1705	–1229	–1484
3.0	0	0.5	272	1192	911	1624
		–0.5	–2607	–1723	–2211	–1646
	π/2	0.5	4058	2027	4306	2071
		–0.5	6277	2461	4510	2074
	π	0.5	843	1487	803	1450
		–0.5	–1320	–1466	–1065	–1348
4.0	0	0.5	258	1136	840	1578
		–0.5	–2651	–1725	–2187	–1632
	π/2	0.5	4134	2047	4416	2076
		–0.5	6471	2475	4600	2079
	π	0.5	376	983	513	1171
		–0.5	–1665	–1440	–1428	1444

TABLE 7

$\tilde{l}$	σ_i^0	ξ	σ_θ^0			
			LP	PNP	GNP	PGNP
2.3	σ_r^0	0.5	78	323	184	476
		–0.5	–14	–265	34	–76
	σ_θ^0	0.5	1453	1834	1546	1785
		–0.5	–2130	–1899	–1471	–1583
2.5	σ_r^0	0.5	64	263	124	1351
		–0.5	–152	–263	–97	–116
	σ_θ^0	0.5	1087	1650	1148	1628
		–0.5	–1580	–1750	–1145	–1494
3.0	σ_r^0	0.5	–150	–225	–73	–2
		–0.5	–226	–200	–87	–135
	σ_θ^0	0.5	857	1300	780	1403
		–0.5	–724	–1388	–548	–906
4.0	σ_r^0	0.5	–306	–725	–4	–146
		–0.5	294	188	283	176
	σ_θ^0	0.5	402	657	328	614
		–0.5	132	–228	28	–195

As the parameter $\tilde{l}$ decreases, the maximum stresses (σ_θ) slightly decrease in the LP (to 7%) and GNP (to 4%) and remain almost constant (difference ≤0.5%) in the PNP and PGNP. The stresses at the center of the bridge for different values of $\tilde{l}$ are much smaller than the maximum stresses on the hole boundaries.

Analyzing the results, we conclude that for $\tilde{l}$ = 2.3, 2.5, 3.0, 4.0 the maximum stresses decrease by 59, 59, 61, and 62% in the PNP, by 27, 27, 28, and 29% in the GNP, and by 66, 66, 67, and 68% in the PGNP compared with the LP.

Conclusions. We have outlined an approach to solving physically and geometrically nonlinear problems of statics for thin shells using three mesh-based methods: FDR, VDM, FEM. Two ways of implementing the Kirchhoff–Love hypotheses have been considered: analytic (algebraic substitution into the formulas for strains) and algorithmic (using Lagrangian multipliers). The VDM and FEM were used as examples to analyze the advantages and shortcomings of these ways.

The analytic implementation of the Kirchhoff–Love hypotheses in the FDM presented no difficulties. This method is expedient to apply to one-dimensional problems. The analytic implementation in the VDM and FEM is more difficult and limits the capabilities of these methods in the case of shells of complex geometry.

The algorithmic implementation based on Lagrangian multipliers is simple and expands the capabilities of numerical methods in the case of nonlinear problems and complex domains. However, it involves some methodological problems

associated with the justification of its application and the possible loss of positive definiteness of the corresponding algebraic systems of equations.

We have numerically solved, as an example, stress-concentration problems for shells made of nonlinear elastic orthotropic composites and elastoplastic isotropic materials.

Note also that the methodological, algorithmic, and analytic aspects in the implementation of the Kirchhoff–Love hypotheses in the theory of thin shells remain to be of current importance, especially for very thin shells. Of interest is joining objects with different number of dimensions (thin shells with rods, three-dimensional bodies, and nonthin shells) described by different types of equations.

REFERENCES

1. N. P. Abovskii, N. P. Andreev, and A. P. Deruga, *Variational Principles in the Theories of Elasticity and Shells* [in Russian], Nauka, Moscow (1978).
2. I. A. Birger, "General methods and algorithms for solving problems of elasticity, plasticity, and creep," in: *Advances in Solid Mechanics* [in Russian], Nauka, Moscow (1975), pp. 51–73.
3. F. K. Bogner, R. L. Fox, and L. A. Schmit, "A cylindrical shell discrete element," *AIAA J.*, **5**, No. 4, 745–750 (1967).
4. D. V. Vainberg, V. M. Gerashchenko, I. Z. Roitfarb, and A. L. Sinyavskii, "Deriving mesh-based equations of bending of plates using a variational method," in: *Resistance of Materials and Theory of Structures* [in Russian], Budivel'nyk, Kyiv (1965), pp. 23–33.
5. K. Washizu, *Variational Methods in Elasticity and Plasticity*, 2nd ed., Pergamon Press, Oxford (1975).
6. K. Z. Galimov, *Fundamentals of the Nonlinear Theory of Thin Shells* [in Russian], Izd. Kazansk. Univ., Kazan (1975).
7. A. I. Golovanov and M. S. Kornishin, *An Introduction to the Finite-Element Method in Statics of Thin Shells* [in Russian],: Izd. Kazan. Fiz.-Tekhn. Inst., Kazan (1990).
8. I. P. Ermakovskaya, V. A. Maksimyuk, and I. S. Chernyshenko, "Nonlinear elastic two-dimensional problems of statics for orthotropic thin shells and a method to solve them," *Red. Zh. Prikl. Mekh*., Kyiv (1988), No. 7526-88 dep. at VINITI 19.10.88, abstracted in. Prikl. Mekh., 25, No. 2, 129 (1989).
9. O. C. Zienkiewicz, *The Finite-Element Method in Engineering Science*, McGraw-Hill, New York (1971).
10. O. C. Zienkiewicz and K. Morgan, *Finite Elements and Approximation*, John Wiley and Sons, New York (1983).
11. A. A. Il'yushin, *Plasticity* [in Russian], Gostekhizdat, Moscow–Leningrad (1948).
12. L. M. Kachanov, *Fundamentals of the Theory of Plasticity* [in Russian], Nauka, Moscow (1969).
13. A. N. Guz, A. S. Kosmodamianskii, V. P. Shevchenko, et al., *Stress Concentration*, Vol. 7 of the 12-volume series *Mechanics of Composite Materials* [in Russian], A.S.K., Kyiv (1998).
14. M. S. Kornishin, *Nonlinear Problems in the Theory of Plates and Shallow Shells and Methods to Solve Them* [in Russian], Nauka, Moscow (1964).
15. V. A. Lomakin, "Theory of anisotropic plasticity," *Vestn. Mosk. Univ.*, *Mat. Mekh*., No. 4, 49–53 (1964).
16. V. A. Lomakin and M. A. Yumashev, "Stress–strain relationships with nonlinear deformation of orthotropic glass-reinforced plastics," *Mech. Comp. Mater*., **1**, No. 4, 15–18 (1965).
17. V. A. Maksimyuk, "Method of Lagrangian multipliers in the theory of shells," *Visn. KNTEU*, No. 2, 91–100 (2008).
18. V. A. Maksimyuk, "Using the method of Lagrangian multipliers in static problems for composite shells," *Dop. NAN Ukrainy*, No. 11, 75–79 (1998).
19. V. A. Maksimyuk, "Successive elimination of Lagrangian multipliers," in: *System Technologies. Mathematical Problems of Engineering Mechanics* [in Ukrainian], Issue 4 (57), Dnepropetrovsk (2008), pp. 45–47.
20. V. A. Maksimyuk, S. A. Silivra, and I. S. Chernyshenko, "Stress distribution in orthotropic shells of revolution with nonlinear factors taken into account," *Teor. Prikl. Mekh*., **18**, 76–78 (1987).
21. V. V. Novozhilov, *Fundamentals of Nonlinear Elasticity* [in Russian], Gostekhizdat, Moscow–Leningrad (1948).
22. V. A. Postnov and I. Ya. Kharkhurim, *Finite-Element Method in Ship Design* [in Russian], Sudostroenie, Leningrad (1974).
23. E. A. Storozhuk, I. S. Chernyshenko, and I. B. Rudenko, "Inelastic deformation of a flexible spherical shell in the form of an eccentric ring," *Teor. Prikl. Mekh*., **43**, 76–81 (2007).

24. A. N. Guz, I. S. Chernyshenko, V. N. Chekhov, et al., *Theory of Thin Shells Weakened by Holes*, Vol. 1 of the five-volume series *Methods of Shell Design* [in Russian], Naukova Dumka, Kyiv (1980).
25. A. G. Ugodchikov and Yu. G. Korotkikh, *Some Methods for Computer Solution of Physically Nonlinear Problems for Plates and Shells* [in Russian], Naukova Dumka, Kyiv (1971).
26. P. M. A. Areias, J.-H. Song, and T. Belytschko, "A finite-strain quadrilateral shell element based on discrete Kirchhoff–Love constraints," *Int. J. Numer. Meth. Eng*., **64**, 1166–1206 (2005).
27. M. E. Babeshko and Yu. N. Shevchenko, "On two approaches to determining the axisymmetric elastoplastic stress–strain state of laminated shells made of isotropic and transversely isotropic bimodulus materials," *Int. Appl. Mech*., **44**, No. 6, 644–652 (2008).
28. T. Belytschko, W. K. Liu, and B. Moran, *Nonlinear Finite Elements for Continua and Structures*, John Wiley & Sons, Chichester (2000).
29. I. S. Chernyshenko, "On the elastic-plastic equilibrium of revolution for finite deflections," *Int. Appl. Mech*., **2**, No. 9, 17–22 (1966).
30. I. S. Chernyshenko, E. A. Storozhuk, and F. D. Kadyrov, "Inelastic deformation of flexible cylindrical shells with an elliptic hole," *Int. Appl. Mech*., **43**, No. 5, 512–518 (2007).
31. I. S. Chernyshenko, E. A. Storozhuk, and S. B. Kharenko, "Elastoplastic state of flexible cylindrical shells with a circular hole under axial tension," *Int. Appl. Mech*., **44**, No. 7, 802–809 (2008).
32. I. S. Chernyshenko, E. A. Storozhuk, and S. B. Kharenko, "Physically and geometrically nonlinear deformation of conical shells with an elliptic hole," *Int. Appl. Mech*., **44**, No. 2, 174–181 (2008).
33. I. S. Chernyshenko, E. A. Storozhuk, and I. B. Rudenko, "Stress–strain state of a flexible spherical shell with an eccentric circular hole," *Int. Appl. Mech*., **43**, No. 10, 1142–1148 (2007).
34. I. S. Chernyshenko and V. A. Maksimyuk, "On the stress–strain state of toroidal shells of elliptical cross section formed from nonlinear elastic orthotropic materials," *Int. Appl. Mech*., **36**, No. 1, 90–97 (2000).
35. I. S. Chernyshenko and V. A. Maksimyuk, "Physically nonlinear deformation of orthotropic shells of revolution," *Int. Appl. Mech*., **22**, No. 1, 42–45 (1986).
36. J. Y. Cho and S. N. Atluri, "Analysis of shear flexible beams, using the meshless local Petrov–Galerkin method, based on a locking-free formulation," *Eng. Comp*., **18**, No. 1–2, 215–240 (2001).
37. E. N. Dvorkin and K.-J. Bathe, "A continuum mechanics based four-node shell element for general nonlinear analysis," *Eng. Comp*., **1**, 77–88 (1984).
38. B. Fraeijs de Veubeke, "A conforming finite element for plate bending," *Int. J. Solid. Struct*., **4**, No. 1, 83–89 (1986).
39. V. P. Georgievskii, A. N. Guz, V. A. Maksimyuk, and I. S. Chernyshenko, "Numerical analysis of the nonlinearly elastic state around cutouts in orthotropic ellipsoidal shells," *Int. Appl. Mech*., **25**, No. 12, 1207–1212 (1989).
40. A. N. Guz, I. S. Chernyshenko, V. P. Georgievskii, and V. A. Maksimyuk, "The stress state of thin-walled elements of structures fabricated from nonlinearly elastic orthotropic composite materials," *Int. Appl. Mech*., **24**, No. 4, 337–343 (1988).
41. A. N. Guz, I. S. Chernyshenko, and K. I. Shnerenko, "Stress concentration near openings in composite shells," *Int. Appl. Mech*., **37**, No. 2, 139–181 (2001).
42. A. N. Guz and P. S. Polyakov, "An experimental study of deformations beyond the elastic limit of spherical bottoms weakened by holes," *Int. Appl. Mech*., **2**, No. 11, 79–81 (1966).
43. A. N. Guz, E. A. Storozhuk, and I. S. Chernyshenko, "Inelastic deformation of flexible spherical shells with two circular openings," *Int. Appl. Mech*., **40**, No. 6, 672–678 (2004).
44. A. N. Guz, E. A. Storozhuk, and I. S. Chernyshenko, "Physically and geometrically nonlinear static problems for thin-walled multiply connected shells," *Int. Appl. Mech*., **39**, No. 6, 679–687 (2003).
45. L. R. Herrmann and D. M. Campbell, "A finite-element analysis for thin shells," *AIAA J*., No. 6, 1842–1847 (1968).
46. L. R. Herrmann, "Finite-element analysis for plates," *J. Eng. Mech. Div. ASCE*, **93**, EM-5, 13–26 (1967).
47. N. H. Kim, K. K. Choi, J.-S. Chen, and M. E. Botkin, "Meshfree analysis and design sensitivity analysis for shell structures," *Int. J. Numer. Meth. Eng*., **53**, 2087–2116 (2002).
48. A. L. Kravchuk, E. A. Storozhuk, and I. S. Chernyshenko, "Stress distribution in flexible cylindrical shells with a circular cut beyond the elastic limit," *Int. Appl. Mech*., **24**, No. 12, 1179–1182 (1988).
49. V. A. Maksimyuk, "Physically nonlinear problems of the theory of orthotropic composite shells with a curvilinear opening," *Int. Appl. Mech*., **34**, No. 9, 835–839 (1998).

50. V. A. Maksimyuk, "Solution of physically nonlinear problems of the theory of orthotropic shells using mixed functionals," *Int. Appl. Mech*., **36**, No. 10, 1349–1354 (2000).
51. V. A. Maksimyuk, "Study of the nonlinearly elastic state of an orthotropic cylindrical shell with a hole, using mixed functionals," *Int. Appl. Mech*., **37**, No. 12, 1602–1606 (2001).
52. V. A. Maksimyuk and I. S. Chernyshenko, "Mixed functionals in the theory of nonlinearly elastic shells," *Int. Appl. Mech*., **40**, No. 11, 1226–1262 (2004).
53. V. A. Maksimyuk and I. S. Chernyshenko, "Nonlinear elastic state of thin-walled toroidal shells made of orthotropic composites," *Int. Appl. Mech*., **35**, No. 12, 1238–1245 (1999).
54. V. A. Maksimyuk and I. S. Chernyshenko, "Physically nonlinear axisymmetrical problems of the theory of orthotropic shells of variable thickness," *Int. Appl. Mech*., **23**, No. 1, 38–41 (1987).
55. V. A. Maksimyuk, S. A. Silivra, and I. S. Chernyshenko, "Stress state of orthotropic thin shells with geometric and physical nonlinearities taken into account," *Int. Appl. Mech*., **24**, No. 8, 763–767 (1988).
56. V. A. Maksimyuk, "Investigating the nonlinearly elastic state of orthotropic shells of revolution on the basis of flow theory," *Int. Appl. Mech*., **34**, No. 8, 786–788 (1998).
57. K. Mallikarjuna Rao and U. Shrinivasa, "A set of pathological tests to validate new finite elements," *Sadhana*, **26**, 549–590 (2001).
58. V. A. Merzlyakov, "Thermoelastoplastic deformation of noncircular cylindrical shells," *Int. Appl. Mech*., **44**, No. 8, 892–904 (2008).
59. G. Prathap, *The Finite Element Method in Structural Engineering*, *Series: Solid Mechanics and Its Applications*, Vol. 24, Kluwer, Dordrecht (1993).
60. V. P. Revenko, "Numerical–analytical method to determine the stress state of an elastic rectangular plate," *Int. Appl. Mech*., **44**, No. 1, 73–80 (2008).
61. N. P. Semenyuk, V. M. Trach, and V. V. Merzlyuk, "On the canonical equations of Kirchhoff–Love theory of shells," *Int. Appl. Mech*., **43**, No. 10, 1149–1156 (2007).
62. E. A. Storozhuk and I. S. Chernyshenko, "Elastoplastic axially asymmetric deformation of shells with curvilinear openings," *Int. Appl. Mech*., **22**, No. 7, 644–649 (1986).
63. E. A. Storozhuk and I. S. Chernyshenko, "Elastoplastic deformation of flexible cylindrical shells with two circular holes under axial tension," *Int. Appl. Mech*., **41**, No. 5, 506–511 (2005).
64. E. A. Storozhuk and I. S. Chernyshenko, "Physically and geometrically nonlinear deformation of spherical shells with an elliptic hole," *Int. Appl. Mech*., **41**, No. 6, 666–674 (2005).
65. E. A. Storozhuk and I. S. Chernyshenko, "Stress distribution in physically and geometrically nonlinear thin cylindrical shells with two holes," *Int. Appl. Mech*., **41**, No. 11, 1280–1287 (2005).
66. E. A. Storozhuk, I. S. Chernyshenko, and V. L. Yaskovets, "Elastoplastic state of spherical shells in the region of an elliptical hole," *Int. Appl. Mech*., **25**, No. 7, 667–672 (1989).
67. E. N. Troyak, E. A. Storozhuk, and I. S. Chernyshenko, "Elastoplastic state of a conical shell with a circular hole on the lateral surface," *Int. Appl. Mech*., **24**, No. 1, 65–69 (1988).
68. I. A. Tsurpal, "Physically nonlinear problems of stress concentration in members, structures, and buildings," *Int. Appl. Mech*., **43**, No. 1, 79–84 (2007).
69. T. M. Wasfy and A. K. Noor, "Computational strategies for flexible multibody systems," *ASME Appl. Mech. Rev*., **56**, No. 6, 553–613 (2003).
70. G. A. Wempner, J. T. Oden, and D. A. Kross, "Finite element analysis of thin shells," *J. Eng. Mech. Div. ASCE*, **94**, EM8, 1273–1294 (1968).
71. S. Wu, G. Li, and T. Belytschko, "A DKT shell element for dynamic large deformation analysis," *Commun. Numer. Meth. Eng*., **21**, 651–674 (2005).
72. V. L. Yaskovets, E. A. Storozhuk, and I. S. Chernyshenko, "Elastoplastic equilibrium of a spherical shell in the form of an eccentric ring," *Int. Appl. Mech*., **26**, No. 1, 56–61 (1990).
73. O. C. Zienkiewicz and R. L. Taylor, *The Finite Element Method*, Vol. 1: *The Basis*, Butterworth-Heinemann, Oxford (2000).
74. O. C. Zienkiewicz and R. L. Taylor, *The Finite Element Method*, Vol. 2: *Solid Mechanics*, Butterworth-Heinemann, Oxford 459 p. (2000).